



# Alterations in Redox Homeostasis and Profound Developmental Consequences Are at the Core of Sudden Gravity Change Responses of Sugarcane Plants

Lucas Felipe da Silva<sup>1,5</sup> · Helaine Cristiane Silva<sup>1,3,4</sup> · Diego Gomes Teixeira<sup>2,4</sup> · Vladimir Vieira do Nascimento<sup>1,3,4</sup> · Kellya Francisca Mendonça Barreto<sup>1,3,4</sup> · Silvia Regina Batistuzzo de Medeiros<sup>3,4,5</sup> · João Paulo Matos Santos Lima<sup>2,5</sup> · Katia Castanho Scortecci<sup>1,3,4,5</sup>

Received: 20 March 2023 / Accepted: 7 October 2023 / Published online: 9 November 2023  
© The Author(s), under exclusive licence to Springer Science+Business Media, LLC, part of Springer Nature 2023

## Abstract

Understanding how abiotic stress influences plant development is important for crop development and management. The gravity changes force may reveal the additional details of the interconnected nature of plants' stress-signaling pathways. Sugarcane plants were submitted to gravity-changing forces using the VSB-30 sounding rocket to identify how these plants respond to this abiotic stress using histological, biochemical, and molecular approaches to evaluate this response. The histological analysis allowed us to observe that this alteration culminates in the intense disorganization of vascular bundles and higher lignin accumulation in plant cell walls at the adaxial epidermis and the mesophyll cells. An increase in enzyme activity from superoxide dismutase and guaiacol peroxidase was also observed. Our results indicate that sugarcane's response is similar to other abiotic stress responses, such as oxidative stress. The RNA sequencing data showed that these plantlets had a different expression on pathways associated with signal perception, plant metabolism involving photosynthesis, amino acid synthesis, cell division, DNA repair, and oxidative enzymes for scavenging ROS. These results presented here using sugarcane plantlets expand our knowledge of how plants can respond to the forces of gravity changes. The expression pattern in roots and leaves showed integrated and distinct responses for some known pathways, and both tissues expressed stress-related transcripts.

**Keywords** Abiotic stress · Change in gravity force · Microgravity · RNA sequence · *Saccharum* spp. · Signal transduction

## Abbreviations

AU	Activity units
APX	Ascorbate peroxidase
AsA	Ascorbic acid
BLAST	Basic Local Alignment Search Tool

BP	Biological processes
BUSCO	Benchmarking Universal Single-Copy Orthologs
CAT	Catalase
CC	Cellular components
DAB	Diaminobenzidine
GO	Gene ontology
H <sub>2</sub> O <sub>2</sub>	Hydrogen peroxide
ISS	International Space Station

Handling Editor: Vijay Pratap Singh.

Lucas Felipe da Silva and Helaine Cristiane Silva have contributed equally to this study.

✉ Katia Castanho Scortecci  
kacscort@yahoo.com; katia.scortecci@ufrn.br

<sup>1</sup> Laboratório de Transformação de Plantas e Análise em Microscopia (LTAPM), Departamento de Biologia Celular e Genética, Centro de Biociências, Universidade Federal do Rio Grande do Norte, Natal, RN, Brazil

<sup>2</sup> Laboratório de Sistemas Metabólicos e Bioinformática (LASIS), Departamento de Bioquímica, Centro de Biociências, Universidade Federal do Rio Grande do Norte, Natal, RN, Brazil

<sup>3</sup> Laboratório de Biologia Molecular e Genômica, Departamento de Biologia Celular e Genética, Centro de Biociências, Universidade Federal do Rio Grande do Norte, Natal, RN, Brazil

<sup>4</sup> Programa de Pós-Graduação em Bioquímica e Biologia Molecular Centro de Biociências, Universidade Federal do Rio Grande do Norte, Natal, RN, Brazil

<sup>5</sup> Programa de Pós-Graduação em Bioinformática, Instituto Metrópole Digital, Universidade Federal do Rio Grande do Norte, Natal, RN, Brazil

KEGG	Kyoto Encyclopedia of Genes and Genomes
LCH	Leaves control in horizontal position
LCV	Leaves control in vertical position
LMH	Leaves VSB-30 flight-submitted in horizontal position
LMV	Leaves VSB-30 flight-submitted in vertical position
MF	Molecular functions
NO	Nitric oxide
PCV	Plantlets submitted to control shaker
POX	Guaiacol peroxidase
RCH	Roots control in horizontal position
RCV	Roots control in vertical position
RIN	RNA integrity number
RMH	Roots VSB-30 flight-submitted in horizontal position
RMV	Roots VSB-30 flight-submitted in vertical position
ROS	Reactive oxygen species
SEM	Scanning electron microscopy
SOD	Superoxide dismutase
UniProtKB	Entry from the UniProt database
1 g	Earth gravity (normal condition)
1 g aM	Sugarcane plant grown after microgravity

## Introduction

Plants are sessile organisms that evolved to grow and develop under different environmental conditions and in the presence of Earth's gravity (1 g) (Hoson 2014). For the last five decades, there has been a particular interest in understanding how plants respond to gravity alterations based on experiments in simulated platforms and biological systems for space cultivation (Baba et al. 2022; Sathasivam et al. 2021). The idea is to use the changes of gravitational force for research to understand how plant responds to this condition to improve yield and to understand plant might grown in this conditions thinking in life in others planets (Zheng et al. 2015; Baba et al. 2022). Many researchers agree that gravity perception occurs through the sedimentation of amyloplasts starch statoliths present in the columella cell from the root cap and hypocotyl endodermis and bundle sheath parenchyma in roots and shoots, respectively (Hashiguchi et al. 2013; Herranz and Medina 2014; Baba et al. 2022). This perception triggers signal transduction pathways, which leads to the organ's orientation and continued growth by cell division. Other hypotheses include the modification in auxin flow within cells, cytoskeleton reorganization by actin filaments and microtubules, and cell division (Herranz and Medina 2014; Kordyum 2014; Ueda et al. 2014; Vandenberg et al. 2014; Baba et al. 2022).

Molecular studies using *Arabidopsis* plants and cell culture showed the participation of several pathways, including calcium, lipid, and pH-related signaling, nitric oxide (NO), and reactive oxygen species (ROS) cascades, growth regulators, cell wall metabolism, and lignin accumulation, secondary metabolism, and changes in post-transcriptional regulation and ribosome turnover. Data from transcriptomic and proteomic experiments from simulated and real microgravity conditions observed that some genes and proteins were differentially expressed, and this information points to general stress response pathways, especially in cell wall (lignin accumulation), plant metabolism (involving auxin stimulus, photosynthesis, ATP synthase, ATP hydrolase, fructose-1,6-bisphosphate aldolase, malate dehydrogenase, calnexin, and others), protein regulation (phosphorylation and dephosphorylation by the activity of different protein kinases and phosphatases), protein degradation using the endoplasmic reticulum pathway (in the CDC48 pathway, Heat Shock proteins), and ROS production and scavenging (accumulation of H<sub>2</sub>O<sub>2</sub> in tissues, activation of different enzymes such as peroxidases, catalase, and others) (Martzivanou et al. 2006; Barjaktarović et al. 2009; Fengler et al. 2015, 2016; Zhang et al. 2015; Beisel et al. 2019; Sathasivam et al. 2021; Baba et al. 2022). However, the precise coordination of how these steps progress in plant cells needs further elucidation.

For that reason, although these changes in gravitational force are not a natural condition, it is also important to understand how plants respond to these stress-induced pathways and their effects on plant development. In addition, these changes in gravitational force can also be compared to other abiotic conditions to identify the similar pathways, as the microgravity response has been associated with an oxidative response.

The present study uses sugarcane plants (*Saccharum* spp. L.) as a plant model due to the genetic information available (transcriptome and partial genome sequence—Vettore et al. 2001; de Setta et al. 2014) and because of its economic importance for sugar and ethanol production in the world. Additionally, our research group has been using sugarcane, a C4 monocot plant, to explore DNA repair, the flowering process, and its oxidative stress response (Medeiros et al. 2019; Morais et al. 2023). Here, 10-day-old sugarcane plants were subjected to changes in gravitational forces (vibration, hypergravity, and microgravity) using the VSB-30 sounding-rocket flight. These plants were analyzed using different approaches such as morphological, biochemical, and molecular techniques, including RNA sequencing. Changes in tissue reorganization for leaves and roots were observed. The biochemical data showed higher activity for SOD and POX enzymes, and bioinformatic data reinforced mRNA expression changes in signal transduction pathways (e.g., inositol monophosphatase family), plant metabolism (e.g.,

photosynthesis, amino sugar and nucleotide sugar metabolism, glyoxylate metabolism, terpenoids metabolism, and others), DNA repair, and other pathways associated with perception, energy, and plant development. The results presented here reinforce the perception and oxidative response. Therefore, it shows an oxidative signaling and transcriptional and post-transcriptional responses associated with changes in gravitational forces for a C4 monocot plant.

## Materials and Methods

### Plant Material

Sugarcane stalks from the SP81-3250 cultivar were grown in a vermiculite substrate in a controlled growth room (temperature  $27 \pm 2$  °C, 70% relative humidity, 12-h photoperiod, and a photon flux density of approximately  $300 \mu\text{mol m}^{-2} \text{s}^{-1}$  at plant level) at coordinates ( $02^\circ 22' 39.52'' \text{ S}$  and  $44^\circ 23' 57.71'' \text{ W}$ ). For VSB-30 flight, sugarcane plants were divided into two boxes: one with the plants fixed in a vertical position (20 plants) and the other in a horizontal position (14 plants). These combinations enabled us to analyze the potential differences in plant acclimation and tissue-specific response.

### Sounding-Rocket Experiment

#### Plants Control

Sugarcane plants exposed to VSB-30 flight were analyzed using different approaches. Considering the transcriptome, the environmental conditions during VSB-30 flight might interfere with expression. Therefore, we used two types of control to mitigate these complex conditions. The first control aimed to simulate similar conditions (time and temperature) to those experienced by the plants during the eight-hour closure in aluminum boxes, both in preparation and during the Maracati II mission flight. To achieve this, sugarcane plants of the same age (10 days old) and height (6 cm) were kept at Earth's gravity (1 g) within aluminum boxes, either in a vertical or in a horizontal orientation, at a temperature of 37 °C for 8 h. The time and temperature were matched to those experienced by the plants during the Maracati II flight. We estimated the time considering the experiment's preparation for the mission, the waiting time until rocket launch, flight, payload recovery, plant sampling, and storage, as described above.

The second control, referred to as the vibration control, was also implemented to address the complex conditions of the VSB-30 flight. For this purpose, we placed 10-day-old, 6-cm-tall sugarcane plants inside the same aluminum box and subjected them to a shaker that simulated the same

vibration and rotation levels experienced by the plants during the VSB-30 flight. We carried out this simulation at the *Instituto Nacional de Pesquisas Espaciais* (INPE—National Institute of Space Research) in São José dos Campos—SP/Brazil (Silva et al. 2011). These two controls (temperature and vibration) were crucial to minimize the interference from environmental conditions during the VSB-30 flight for transcriptome analysis through bioinformatic analysis.

### VSB-30 Experiment Preparation

The experiment was part of the Brazilian microgravity program—Maracati II mission on December 12<sup>th</sup>, 2010 (VSB-30 sounding rocket), with a flight duration of 18 min, reaching an apogee of 241.9 km and experiencing 6 min of microgravity. We placed the sugarcane plants in two hermetic aluminum boxes designed to minimize stress conditions, as detailed by Silva et al. (2011). Throughout the VSB-30 flight, these plants underwent 8 g of force for one second (hypergravity) and the experienced microgravity ( $10^{-6}$  g) for 6 min. Each box was equipped with two data loggers (NOVUS, Paraná, PR, Brazil) that recorded temperature and humidity every 10 s during the experimental period. One box contained 14 plants positioned horizontally, while the other held 20 plants in a vertical orientation. The average temperature during the 18-min VSB-30 flight was 37 °C.

Once the payload was retrieved from the sea, it was transported to Santana Island, where our experimental team opened the boxes. Leaves and roots were subsequently isolated and placed in an RNAlater solution (Ambion) or an FAA solution (1 formaldehyde: 18 ethanol: 1 acetic acid) for histological analysis. Samples intended for RNA and protein analysis were stored at  $-80$  °C until use. Furthermore, following the flight and payload recovery, one randomly selected vertically oriented plant was planted in soil (1 g aM—after microgravity) to assess the long-term effects on later plant development.

The entire experiment, encompassing plant preparation, sample loading into the two boxes, flight, payload recovery, and isolation of tissues (leaves and roots), spanned a total of 8 h. Throughout these 8 h, the sugarcane plants remained inside the aluminum boxes, with the data loggers continuously temperature and humidity.

### Histological Analysis

To describe the morphological responses to microgravity, leaf and root tissues were assessed through light microscopy and scanning electron microscopy (SEM) analysis. We examined three groups: control plants not subjected to the VSB-30 flight, plants exposed to the VSB-30 flight in both horizontal and vertical orientation, and a plant maintained under 1 g conditions after the flight (1 g aM plants).

## Light Microscopy

Plants intended for histological analysis (light microscopy or SEM) were immersed in an FAA solution for 48 h and subsequently transferred to a 70% ethanol solution for preservation until future analysis. Fragments of both leaves and roots were embedded in wax, and 5- $\mu\text{m}$  sections were obtained following the procedure described by Langdale (1994). These sections were then stained using toluidine blue, safranin-O, and diaminobenzidine (DAB) as outlined by Langdale (1994). The toluidine blue and safranin-O dyes facilitated the lignin accumulation, while DAB indicated the presence of hydrogen peroxide ( $\text{H}_2\text{O}_2$ ) accumulation in tissues through a brown–red coloration.

Image capture was conducted using Olympus microscopy with a DXM1200 Nikon camera and Nikon ACTL software. For all light microscopy analyses, triplicate samples were used each replicate.

## Scanning Electron Microscopy (SEM)

Root and leaf samples were affixed to carbon stubs using carbon tape and silver conductive epoxy (Agar). Subsequently, the samples underwent vacuum and were subjected to metalization using SCD-005-BAL-TEC equipment. The resultant images were examined utilizing a SEM XL-30-ESEM-Philips. For all SEM analyses, triplicate samples were employed from each replicate.

## Protein Extraction and Enzyme Activity Assessment

For the extraction of total soluble protein, 250 mg of frozen tissues (leaves or roots) was pulverized into a powder using liquid  $\text{N}_2$  and subsequently placed into tubes containing 1200  $\mu\text{L}$  of a 100 mM potassium phosphate buffer, pH 7.0. This buffer contained 1 mM EDTA and 0.5 mM ascorbic acid, and the mixture was kept on ice for 5 min. Following this, the extracts were subjected to centrifugation for 20 min at 13,000 $\times g$  at 4 °C. The resulting supernatant was carefully transferred to a new tube and utilized for the enzymatic assays. The total protein content was quantified using the Bradford method (Bradford 1976).

Superoxide dismutase (SOD) activity was conducted following the protocol by Torres et al. (2014). Plant extracts aliquots were transferred to 96-well plates containing a 50 mM potassium phosphate buffer at pH 7.8, containing 0.1 mM EDTA, 13 mM L-methionine, and 750  $\mu\text{M}$  Nitroblue tetrazolium (Sigma Aldrich, Saint Louis, MA, USA). The reaction was initiated by adding 2  $\mu\text{M}$  riboflavin (Sigma Aldrich, Saint Louis, MA, USA) to each well, and the plate was exposed to a light source (30 W fluorescent lamp) for 2 min. Absorbance was measured at 560 nm, and the total activity was expressed in Activity Units per minute per

milligram of protein ( $\text{AU min}^{-1} \text{mg}^{-1} \text{Protein}$ ). Ascorbate peroxidase (APX) activity was assessed according to the method outlined by Cavalcanti et al. (2007). Briefly, aliquots of extracts were added to a reaction mixture composed of a 50 mM phosphate buffer pH 6.0, 30 mM ascorbic acid (AsA), and 20 mM  $\text{H}_2\text{O}_2$ . The absorbance was measured at 290 nm was monitored every 30 s for 5 min. Activity was calculated using the molar extinction coefficient for ascorbate ( $A_{290} \text{AsA} = 2.8 \text{mM}^{-1} \text{cm}^{-1}$ ) and expressed in micromoles of  $\text{H}_2\text{O}_2$  decomposed per minute per milligram of protein ( $\mu\text{mol H}_2\text{O}_2 \text{min}^{-1} \text{mg}^{-1} \text{Protein}$ ). Catalase (CAT) activity was determined following the method described by Havir and McHale (1987). Protein extracts were mixed with a 50 mM potassium phosphate buffer at pH 7.0, containing 20 mM  $\text{H}_2\text{O}_2$ . The decrease in absorbance at 240 nm at 30 °C every 30 s for 5 min. Enzymatic activity was calculated using a molar extinction coefficient of 40  $\text{mM}^{-1} \text{cm}^{-1}$  ( $A_{240} \text{H}_2\text{O}_2$ ) and expressed as micromoles of  $\text{H}_2\text{O}_2$  decomposed per minute per milligram of protein ( $\mu\text{mol H}_2\text{O}_2 \text{mg}^{-1} \text{Protein min}^{-1}$ ). Guaiacol peroxidase (POX) activity was determined as outlined by Cavalcanti et al. (2007). A 25  $\mu\text{L}$  portion of the protein extract was combined with a reaction mixture consisting of 50 mM potassium phosphate buffer at pH 6.8, 20 mM guaiacol, and 20 mM  $\text{H}_2\text{O}_2$ . Following a 10-min incubation at 30 °C, the reaction was halted by adding 5% (v/v)  $\text{H}_2\text{SO}_4$ , and absorbance was measured at 480 nm (Urbanek et al. 1991). One POX activity unit (AU) was defined as the change of 1.0 absorbance unit per milliliter of enzymatic extract and expressed as  $\text{AU mg}^{-1} \text{Protein min}^{-1}$ .

## Statistical Analysis

We employed triplicates samples for each analysis in all biochemical assays. The collected data were subjected to significance analysis using ANOVA, and the means ( $\pm\text{SD}$ ) are depicted in the final plots. Disparities between means were evaluated through Tukey post hoc test with a significance level set at 5% probability ( $p \leq 0.05$ ).

## RNA Extraction and Transcriptomic Analysis

Total RNA was extracted from 300 to 500 mg of leaves or roots using an RNeasy Plant Mini Kit (Quiagen, Germany), following the provided manufacturer's guidelines. Ten micrograms of total RNA was subjected to DNase I treatment (TURBO DNA-free Kit, Ambion, TX, USA). Subsequent to the digestion step, RNA quality was assessed using a BioAnalyzer (Agilent, Santa Clara, CA, USA), following the manufacturer's protocol. Total RNA from each sample, possessing a RIN (RNA integrity number) quality value of 8.0 or 9.0, was submitted for RNA sequencing on the Illumina platform.



## Alignment, Assembly of the New Genome, and Annotation of Transcripts

The obtained data were validated using the NGS QC Toolkit package (<http://www.nipgr.res.in/ngsqc toolkit.html>) (Patel and Jain 2012) through the IlluQC.pl script. The raw RNA sequences from the nine experiment-generated libraries were individually analyzed in multiple steps using specific software tools. To assess sequence quality, FastQC software version 0.10.1 (<https://www.bioinformatics.babraham.ac.uk/projects/fastqc/>) (Wingett and Andrews 2018) was employed. Subsequently, CutAdapt (<http://pypi.python.org/pypi/cutadapt>) (Martin 2011) was used to identify and eliminate low-quality sequences and adapter remnants. For mapping, the sequences were aligned against both the *Sorghum bicolor* genome, as a reference, and sugarcane sequences (both from NCBI—<https://www.ncbi.nlm.nih.gov/>) (Sayers et al. 2022) using HiSat2 software (Kim et al. 2015). SAMtools (Li et al. 2009) facilitated the manipulation and conversion of alignment data from SAM to BAM format.

Transcriptome de novo assembly was executed with Trinity software (Grabherr et al. 2011), utilizing BAM files as input. Output files, including FASTA sequences, were subsequently used for transcript annotation via the Benchmarking Universal Single-Copy Orthologs (BUSCO) software (Simão et al. 2015). The chosen parameters involved the Liliopsida lineage dataset, sourced from OrthoDB v10.1 (<https://www.orthodb.org/>) (Zdobnov et al. 2021). The amino acid sequences derived from prediction were analyzed using DIAMOND (Buchfink et al. 2015), which compared against various protein amino acid sequences via BLAST, allowing for name identification.

All these analyses and assembly steps were conducted on the supercomputer located at the High-Performance Processing Center (NPAD) of the Universidade Federal do Rio Grande do Norte (UFRN).

## Functional Analysis and Protein–Protein Interaction Analysis

The transcripts identified in the previous step were compared using VENN diagrams, a web tool available at <http://bioinformatics.psb.ugent.be/beg/tools/venn-diagrams>. This aided in segregating the unique transcripts exclusive to each data library and identifying transcripts common among them. Subsequently, the unique transcripts from each library were mapped to standard identifiers, specifically UniProtKB entries from the UniProt database. This was accomplished with the Retrieve/ID mapping (<https://www.uniprot.org/uploadlists/>) (The UniProt Consortium 2022).

The unique transcripts from each library underwent functional analysis based on gene ontology (GO) categories, encompassing biological processes (BP), cellular

components (CC), and molecular functions (MF). To achieve this, we utilized the GO enrichment module within the PlantRegMap platform, accessible at <http://plantregmap.cbi.pku.edu.cn/> (Tian et al. 2020) with reference parameters for *Sorghum bicolor* and a significance threshold  $p$ -value  $\leq 0.05$ . Additionally, to identify the enriched metabolic pathways specific to each of the libraries, we utilized the functional enrichment module on the KOBAS 3.0 web server, available at <http://kobas.cbi.pku.edu.cn/kobas3> (Xie et al. 2011), which draws from the Kyoto Encyclopedia of Genes and Genomes (KEGG) database (Kanehisa and Goto 2000) using *Sorghum bicolor* as the species reference. To visualize and analyze the enrichment outcomes and unique genes linked to enriched metabolic pathways, we employed the R ggplot2 package (<https://ggplot2.tidyverse.org>) (Wickham 2016).

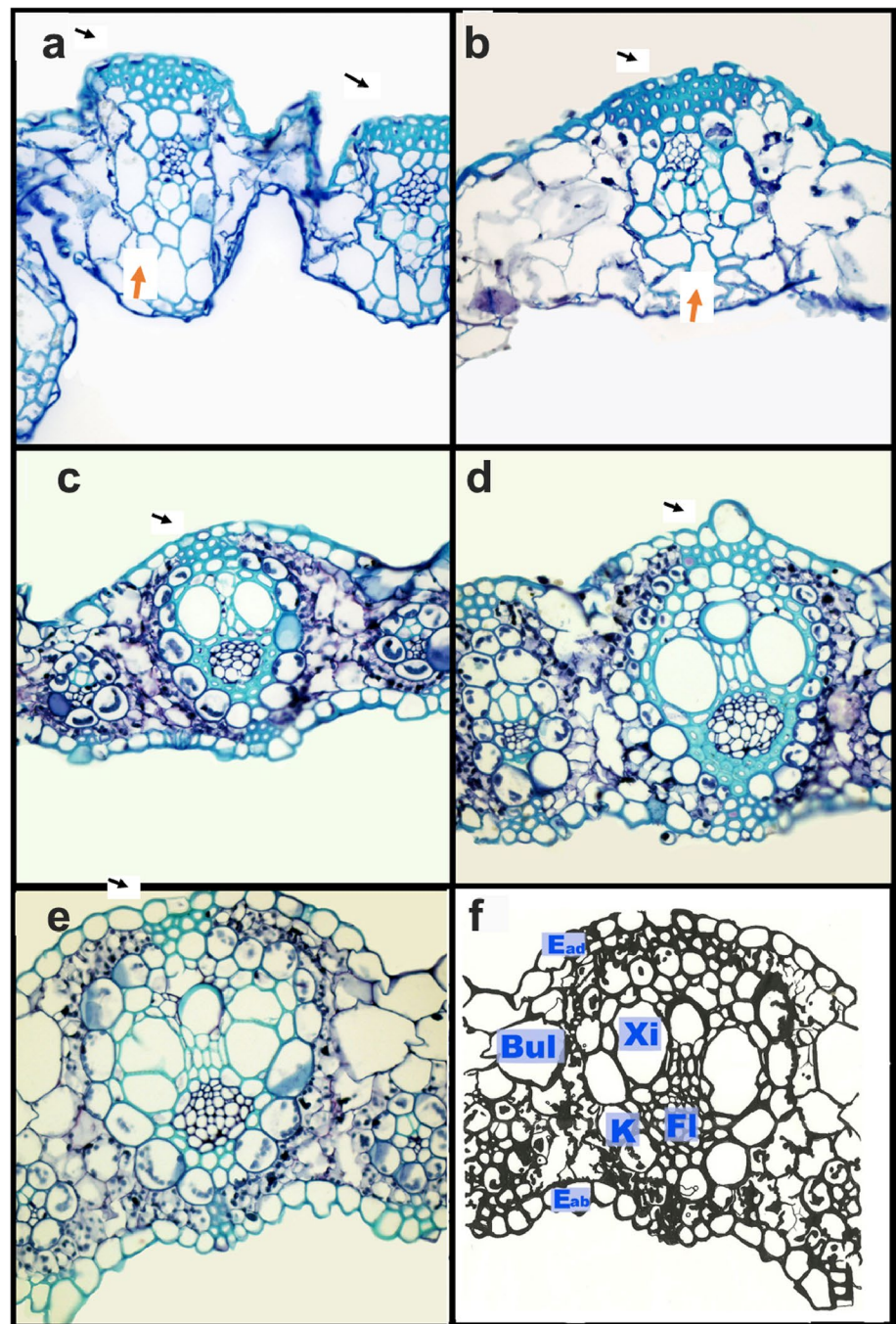
## Results

### Histological Analysis

The toluidine blue staining (Fig. 1) reveals noticeable disorganization in sugarcane leaf tissues, both from vertically and from horizontally positioned plants (Fig. 1a, b), when compared to the control plants (Fig. 1e). Under VSB-30 flight conditions, the bulliform cells (Bul) displayed expansion. Further alterations included modifications in the plant cell wall and lignin accumulation (indicated by black arrow) within the adaxial epidermis (Ead) and the mesophyll cell. Additionally, a complete disruption of vascular bundle organization was observed (indicated by red arrow), affecting xylem and phloem structures. Notably, no discernible differences were observed between vertically and horizontally oriented plants. As anticipated, the control sugarcane plants did not exhibit these observed changes. The schematic representation in Fig. 1f outlines the typical tissue organization and regions found in sugarcane leaves.

The 1 g aM plants also displayed noticeable increases in lignin content in the Ead region (Fig. 1c, d) when compared to the 1 g control plants (Fig. 1e). Furthermore, the Kranz anatomy and organization of vascular bundles were distinct from the plants subjected to the VSB-30 flight conditions (Fig. 1a, b). These flight-exposed plants exhibited some degree of tissue reorganization. However, substantial structural disparities remained evident contrasted with the 1 g control plant (Fig. 1e). Similar outcomes were observed with Safranin-O (Fig. S2). To assess whether the anatomical changes were linked to ROS signaling and production, diamino benzidine (DAB) staining was conducted (Fig. S2). H<sub>2</sub>O<sub>2</sub> accumulation, denoted by a brown–red coloration (black arrow), was apparent around the endodermis and vascular bundles in leaves from plants subjected to the VSB-30 flight (Fig. S2a and 2d), distinct from the relatively inconspicuous

**Fig. 1** Leaf tissues were stained with toluidine blue and observed under 40× magnification. Sections of 5 μm from leaf were subjected to toluidine blue staining. In images **a–d**, leaf tissue samples were extracted from sugarcane plants exposed to the VSB-30 flight conditions. **a** Vertically oriented plants. **b** Horizontally oriented plants. **c** and **d** Tissue from the VSB-30 flight-exposed samples and a vegetative bud, respectively, from a plant that grew for 1 year after the experiment. **e** Control plants that were not subjected to gravitational changes. Additionally, **f** A schematic representation outlining the typical organization of a sugarcane leaf. The black arrow indicates lignin accumulation, while the red arrow highlights the lost the tissue organization (Color figure online)



staining in control plant (Fig. S2e). Notably, there were no significant differences observed in DAB staining between vertically and horizontally oriented plants exposed to the VSB-30 flight.

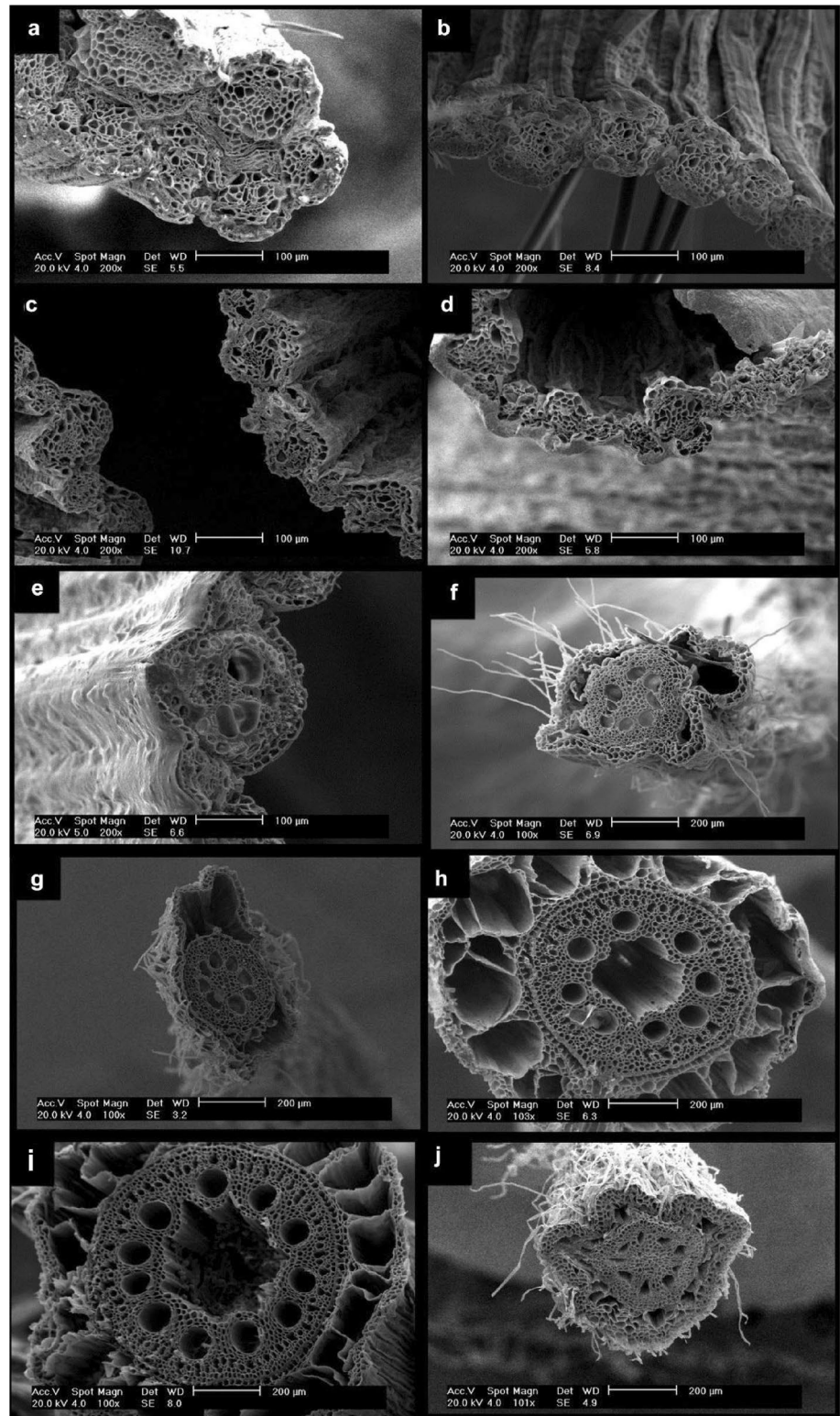
SEM analysis further corroborated the findings from light microscopy. Leaf tissue displayed consistent disorganization (red arrow), irrespective of their vertical or horizontal arrangement within the experimental setup

(Fig. 2a, b, respectively). These alterations persisted partially, as they were still evident in the 1 g aM plant (Fig. 2c) and its vegetative bud (Fig. 2d). Furthermore, the arrangement of xylem and phloem in these samples differed from that in the control plants (Fig. 2e).

Similar patterns were observed in sugarcane root tissues, featuring significant increases in the epidermal layer and metaxylem count across all plants exposed



**Fig. 2** SEM analysis of sugarcane leaf and roots sections. **a** The leaf samples from vertically oriented plants. **b** Samples from horizontally orientated plants. **c** Samples from a 1-year-old sugarcane plant that underwent microgravity exposure during flight conditions subsequently grew under Earth conditions (1 g aM plant). **d** Vegetative propagation from plants described in **c**. **e** A leaf section from control plant. The scale bars in images a–e denote 100  $\mu$ m. For roots: **f** the root samples from vertically oriented plants, and **g** root samples from horizontally oriented plant. **h** Roots samples from a 1-year-old sugarcane plant that experienced microgravity exposure during flight conditions and later grew under Earth conditions (1 g aM plant). **i** Vegetative propagation from the plants described in **h**. **j** A root section from control plants. The scale bars in images f–j correspond to 200  $\mu$ m



to VSB-30 flight (Fig. 2f–i) contrasting with the control plant (Fig. 2f). Intriguingly, our observations indicated an aerenchyma-like aspect in the epidermal layer.

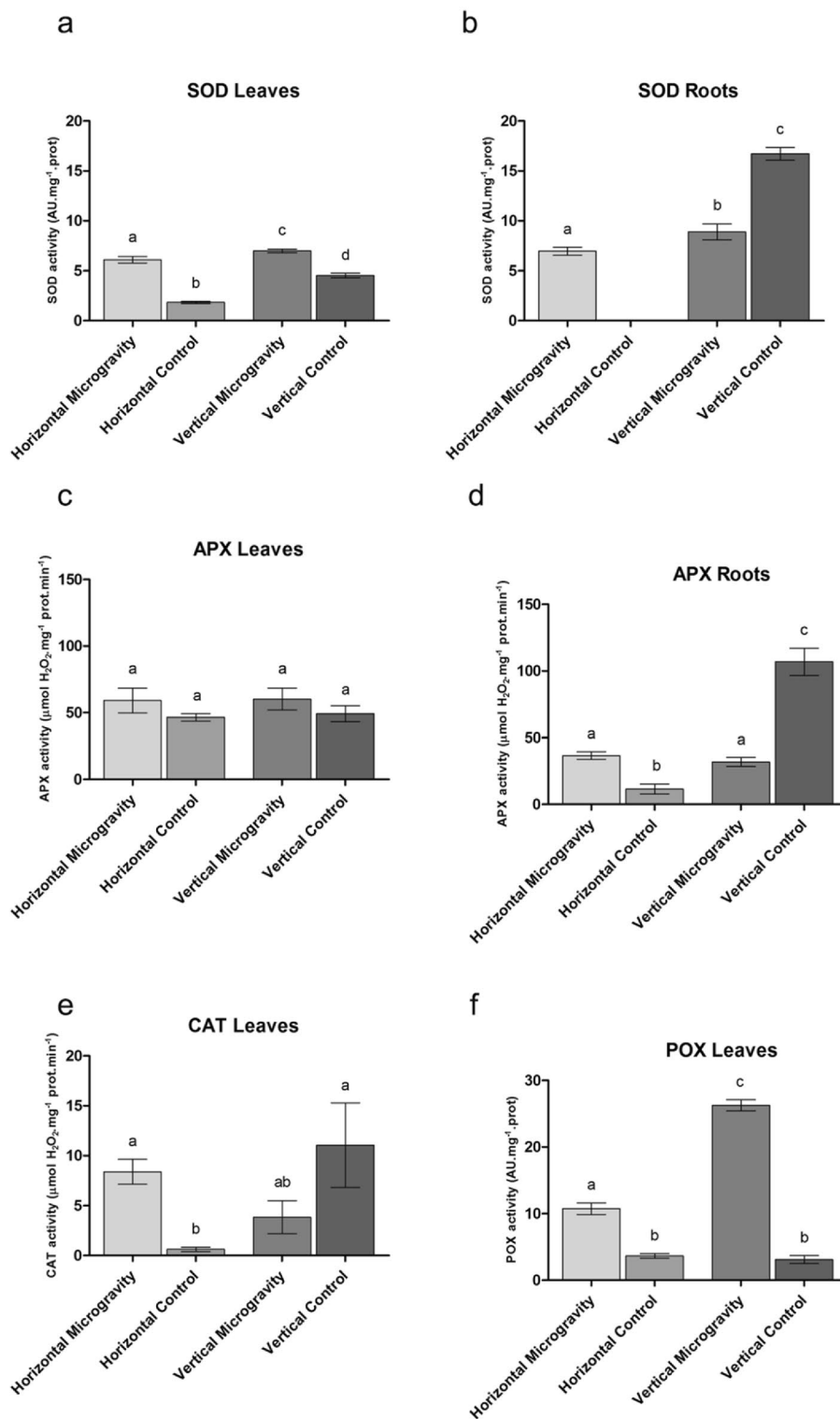
Additionally, the 1 g aM plant exhibited a degradation of the central medullary region, an uncommon occurrence in sugarcane plants.

## Biochemistry Assays

Since we observed a noticeable accumulation of  $H_2O_2$  in sugarcane tissues induced by microgravity, we proceeded to analyze the enzymatic activities of SOD, CAT, APX,

and POX in both leaf and root extracts (Fig. 3). This analysis aimed to gain insights into the response of the antioxidant system. Leaves from plants subjected to the VSB-30 flight conditions (both horizontally and vertically oriented) exhibited significant increases in SOD activity compared

**Fig. 3** Enzymatic activities. **a** SOD activity in leaves, **b** SOD activity in root tissues. APX activities in leaves (**c**) and roots tissues (**d**). CAT (**e**), and POX (**f**) activities in leaf tissues. The bars indicate the standard deviation of three independent replicates. Different letters indicate statistically significant differences ( $p \leq 0.05$ )





to the control plants (Fig. 3a). Conversely, the activities of leaf APX remained relatively consistent across the various tested conditions (Fig. 3c). However, the orientation of the plants affected SOD and APX activities in roots (Fig. 3b, d). Regarding SOD, we observed a noteworthy decrease in root samples from vertically placed plants (Fig. 3b), while APX activity displayed an increase in horizontally oriented plants and a decrease in vertically oriented ones (Fig. 3d).

Similar to the APX activity trends, leaves from horizontally oriented plants exhibited enhanced CAT enzyme activity compared to the control group. However, there were no significant differences observed in leaves from plants subjected to vertical orientation. It's important to note that CAT activity in root tissues was not detected in our assays (data not shown). Another antioxidant enzyme assessed was POX. The data (Fig. 3e) demonstrated a substantial increase in POX activity in leaves exposed to the VSB-30 flight conditions. Although this effect was observed in both horizontal and vertical orientations, it was more pronounced in vertically oriented plants. These findings underscore the fact that changes in gravitational force stimuli due to the VSB-30 flight significantly modulated the activity of certain enzymatic antioxidant systems, with this modulation being tissue-specific.

## RNA Expression Pattern

To gain insights into the molecular responses of sugarcane plants exposed to the VSB-30 flight, we generated and sequenced nine cDNA libraries using the Illumina HiSeq 2000 platform. Four of these libraries encompassed plant tissues (roots and leaves) subjected to the VSB-30 flight (M) in either horizontal or vertical positions: roots VSB-30 flight-submitted in horizontal position (RMH), leaves VSB-30 flight-submitted in horizontal position (LMH), roots VSB-30 flight-submitted in vertical position (RMV), and leaves VSB-30 flight-submitted in vertical position (LMV) (Table S1). Additionally, we included five control libraries: roots control in horizontal position (RCH), leaves control in horizontal position (LCH), roots control in vertical position (RCV), leaves control in vertical position (LCV), and plantlets submitted to control shaker (PCV) (Table S1). Detailed information about the total number of transcripts within each library can be found in Tables S1 and S2. The assembled contigs ranged from 44,076 to 59,851, with sizes spanning from 201 bp to 11,551 bp (Table S2). An overview of the transcriptome assembly is presented in Fig. 4 that depicts the total, mapped, and non-mapped transcripts (Fig. 4a) as well as the sizes of the obtained (Fig. 4b) for each library.

We conducted similarity searches of the assembled contigs against the *Sorghum bicolor* genome as a reference (Fig. S3). Across all the libraries, complete and single-copy contigs constituted 32.1–42.9% of the total contigs, while

complete and duplicated contigs ranged from 10.3 to 15.7%. The proportion of incomplete contigs varied from 9.8 to 14.8%, with sequences lacking similarity (missing) making up 31.4–43.1%. Given the incomplete nature of the sugarcane genome, these proportions were within the anticipated range, accounting for the genetic divergence between these two crops. From the set of complete and fragmented contigs, we identified 2839 unique UniProtKB entries (Table 1). Although the total number of transcripts in the nine libraries was similar, the count of unique sequences ranged from 282 in LMV to 406 transcripts in RMV, representing the lowest and highest values, respectively.

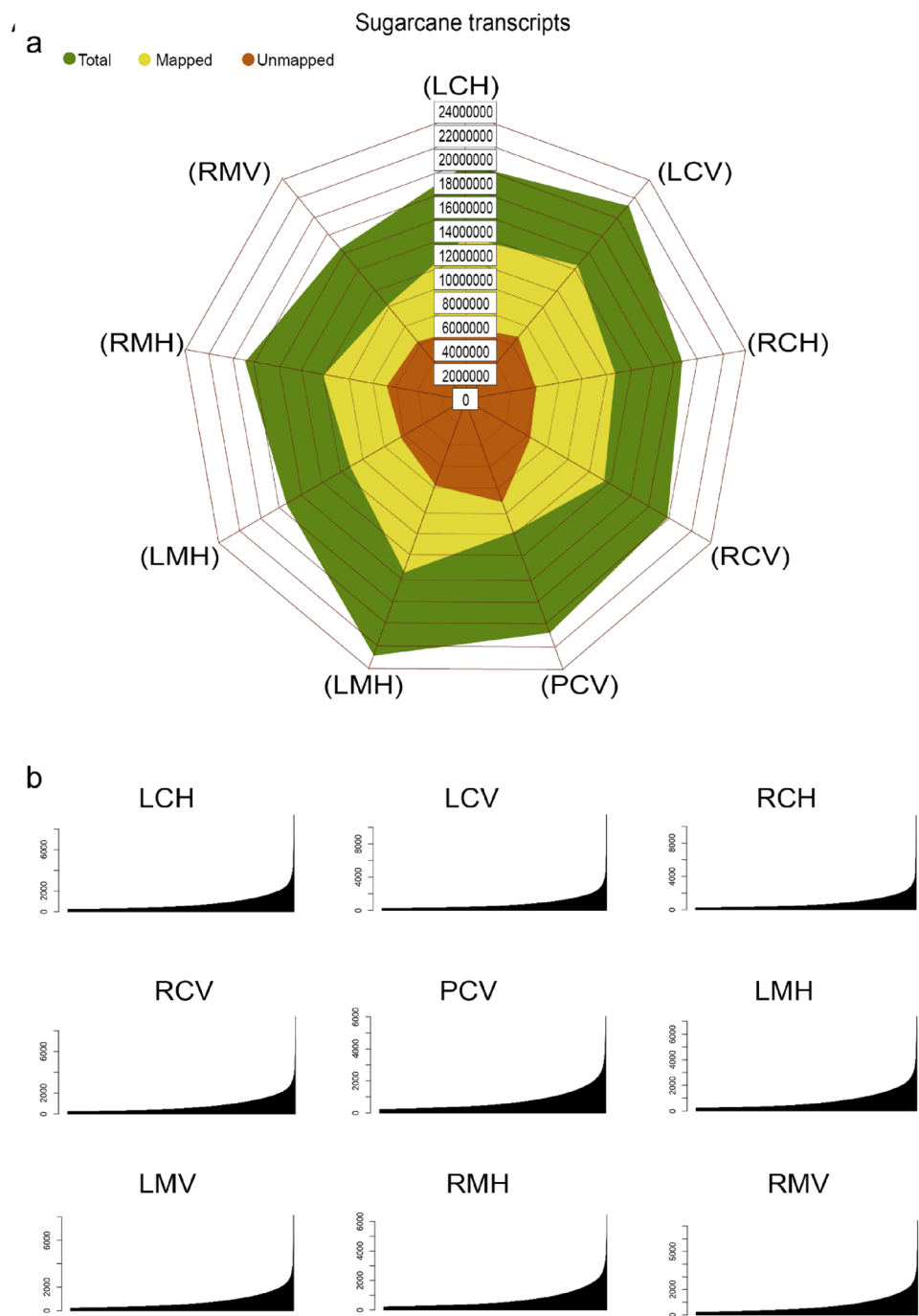
## Functional Analysis

To comprehend the linkage between the acquired transcripts and sugarcane response to the VSB-30 flight conditions, we conducted a GO analysis and linked them to potential metabolic pathways. After undergoing the GO terms enrichment analysis using the PlantRegMap platform, the most prevalent categories were BP and MF. Interestingly, the CC category was infrequent or absent (Table 2), primarily represented in the PCV, LMH, and LMV libraries. The GO analysis also identified 26 transcripts from the LCH library (8.39%) associated with “catalytic activity” MF, and 1.39% of the transcripts from LCV samples linked to terms like “multi-organism reproductive process,” “cell differentiation,” and “cellular developmental process” (Table 2). The RCH featured two transcripts (0.8%) classified under BP category of “glutathione metabolic process,” “cellular modified amino acid metabolic process,” and “sulfur compound metabolic process” (Table 2). Other terms noted in control libraries encompassed “protein binding” MF (RCV library) and “cell part,” and “cell” from the CC category (PCV library) (Table 2).

For the libraries generated VSB-30 flight-exposed sugarcane plants, we observed specific transcript distributions in various categories. In the MF category, the RMH library exhibited twenty-four transcripts (5.91%) associated with the terms “heterocyclic compound binding” and “organic cyclic compound binding.” In the same category, the LMH library contained twelve transcripts (3.78%), with categorization into the CC category where the term “nucleus” was prevalent. Moreover, the RMV library contained ten transcripts (2.9%) classified under the BP category, enriched with terms like “cellular component organization” and “component organization or biogenesis.” The LMV library had thirty transcripts (10.64%) classified under the CC classification, featuring enriched terms “cell part” and “cell” (Table 2).

Furthermore, we identified distinct terms that were exclusive to each library, as depicted in Fig. 5. Specifically, in leaf tissues, the LMV library (Fig. 5a) had 19 unique terms, while the LMH library (Fig. 5b) had 50, when compared

**Fig. 4** Overview of the sugarcane transcriptomes assemblies under control and VSB-30 flight-submitted conditions. **a** Raw data mapping from RNA-seq data depicting the total number of transcripts (dark green regions), the number of mapped transcripts (light green), and the number of non-mapped transcripts (brown), using the *Sorghum bicolor* genome as a reference. **b** Contig size distributions of libraries after de novo assembly using Trinity software (Color figure online)



against the control libraries (PCV, LCV, and LCH). In a similar manner, the root tissue libraries RMV (Fig. 5c) and RMH (Fig. 5d) exhibited 37 and 83 exclusive terms, respectively. When focusing solely on the libraries derived from VSB-30 flight-exposed sugarcane tissues, a comparison revealed 19 specific terms for the LMV library and 35 for LMF. Conversely, the RMV and RMH libraries featured 26 and 66 unique terms, respectively (as depicted in Fig. 5e). Further details about these exclusive terms for each library can be found in Table S3.

Regarding the ontology of BP, the prevalent terms for each library derived from flight-exposed tissues were as follows: RMV—“epidermal development and differentiation,” “DNA organization,” “Golgi vesicle transport,” and “protein modification”; RMH—“signal transduction pathways,” “molecule transport through membrane,” “ATPase metabolism,” “DNA metabolism/DNA repair,” and “RNA metabolism”; LMV—“signal response to hormone or oxidative stress,” “primary metabolism,” and “RNA metabolism”; and LMH—“plant development,” “cell morphogenesis,” and

**Table 1** Number of annotated transcripts in the nine libraries comprising control and VSB-30 flight-submitted sugarcane plants

Library	Total transcripts	Transcripts duplication	Unique transcripts
LCH	9.519	6.906	310
LCV	9.509	6.955	297
RCH	9.015	6.705	250
RCV	9.008	6.755	283
PCV	8.478	6.524	350
LMH	9.629	6.947	317
LMV	8.843	6.682	282
RMH	8.734	6.435	406
RMV	8.529	6.463	344
Total	81.264	60.372 (12.299)	2.839

Values correspond to the total number of transcripts identified in all libraries, duplicated transcripts, and unique transcripts for each specific library.

**Table 2** Transcripts identified and classified according to GO annotation

Library	Transcripts with GO annotation	Transcript after enrichment	CC (%)	MF (%)	BP (%)
LCH	41	61	26.23	55.74	18.03
LCV	33	27	–	7.41	92.59
RCH	23	4	–	25	75
RCV	41	13	7.69	46.15	46.15
PCV	50	40	27.5	17.5	55
LMH	44	55	3.64	7.27	89.09
LMV	45	21	14.28	28.57	57.14
RMH	45	86	13.95	20.93	65.12
RMV	53	39	2.56	17.95	79.49

CC, MF, and BP represent the GO categories of Cellular Components, Molecular Function, and Biological Processes

*LCH* Leaves control in horizontal position, *LCV* Leaves control in vertical position, *RCH* Roots control in horizontal position, *RCV* Roots control in vertical position, *PCV* Plantlets submitted to control shaker, *LMH* Leaves VSB-30 flight-submitted in horizontal position, *LMV* Leaves VSB-30 flight-submitted in vertical position, *RMH* Roots VSB-30 flight-submitted in horizontal position, *RMV* Roots VSB-30 flight-submitted in vertical position

“meristem growth and differentiation.” Figure 6 provides an overview of the terms proportions alongside their respective corrected *p*-values. When considering each flight-submitted library in comparison with its corresponding controls, distinctive profiles emerged. The RMH library displayed terms associated with Selene compound metabolism, ribosome biogenesis, protein processing at the endoplasmic reticulum, and DNA repair. Conversely, the RMV library feature terms linked to amino acid metabolism and pyrimidine, fatty acid

elongation and DNA replication, plant–pathogen interaction or stress response, terpenoid backbone biosynthesis, pentose phosphate pathways, RNA transport, and inositol phosphate metabolism.

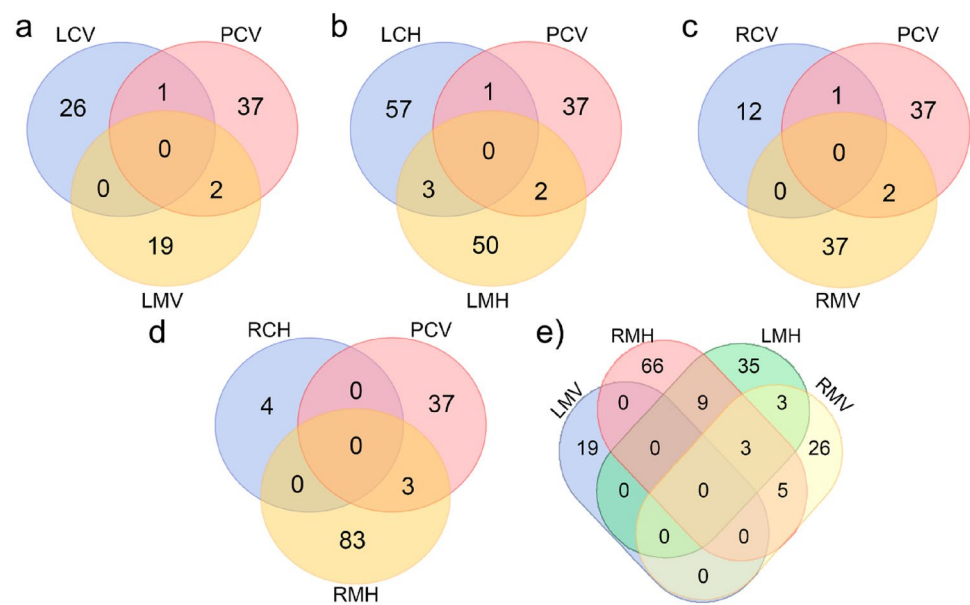
Similarly, leaf tissue libraries exhibited profiles as well. Notably, the LMH library featured terms associated with amino acid metabolism, sulfur metabolism, riboflavin metabolism, inositol phosphate metabolism, purine metabolism, pyruvate metabolism, glycolysis and carbon metabolism, and Biosynthesis of secondary metabolites. On the contrary, the LMV presented a more concise set of terms, including biosynthesis of secondary metabolites, signal pathways (MAPKs), metabolic pathways, and RNA transport. The outcomes depicted in Fig. 6, Table 2, and Table S3 underscore that each tissue type (root or leaf) and orientation (horizontal or vertical) respond uniquely to the altered gravitational force during the VSB-30 flight.

Furthermore, we examined the genes linked to the aforementioned terms and pathways (Table 3). The RMH library had four genes—*C5WVD4*, *C5YNU8*, *C5YSD9*, and *C5WTC1*; four genes to RMV—*C5YLK6*, *C5WYL6*, *C5XMX5*, and *C5YL06*; four genes to LMH—*C5YLK6*, *C5YT78*, *C5Z498*, and *C5YBC8*, and two genes associated to LMV—*C5WZU7* and *C5WLY2*. Furthermore, the gene *C5WYL6* was present in two metabolic pathways: purine metabolism and fatty acid elongation (Table 3). We also assessed the transcripts present in both roots and leaves from the same plant, which could potentially indicate a synchronized response throughout the entire plant. RMV and LMV libraries had terms associated with two metabolic pathways in common: “amino sugar and nucleotide sugar metabolism” and “biosynthesis of secondary metabolites” (Fig. 5e). The pathway “RNA transport” occurred in two distinct flight-submitted leaf tissues libraries: LMH (*A0A1Z5R6U1*) and LMV (*C5YWA7*). In addition, we also evidenced some metabolic pathways shared by other libraries, such as the “phosphatidylinositol signaling system,” identified in the RMV (*C5YT79*), LMH (*C5YT78*), and RCV libraries (*C5XN41*). Similarly, we identified distinct genes associated with the “amino sugar and nucleotide sugar metabolism” pathway from different libraries: RMV (*C5Y5V0*), LMV (*C5WZU7*), and RMH (*C5XQI8*) and in the control library RCH (*C5WZT3*). Another metabolic pathway observed in different libraries was “purine metabolism” expressed in RMV (*C5WYL6*), LMH (*C5WPQ9*), and LCH (*C5WRD4*) (Table 3).

Table 3 lists 22 genes identified in both horizontal and vertical leaf libraries, as well as in horizontal and vertical root libraries during the VSB-30 flight. Due to the lack of a complete sugarcane genome, we utilized sequence databases from *Sorghum bicolor* and *Zea mays*. Some sequences matched uncharacterized proteins within the UniProt database for *Sorghum bicolor*. Subsequently,



**Fig. 5** Venn diagrams illustrating the enriched GO terms for each library. **a** Leaves VSB-30 flight-submitted in vertical position (LMV) compared to the controls (LCV and PCV). **b** Leaves VSB-30 flight-submitted in horizontal position (LMH) compared to controls (LCH and PCV). **c** Roots VSB-30 flight-submitted in vertical position (RMV) compared to the controls (RCV and PCV). **d** Roots VSB-30 flight-submitted in horizontal position (RMH) compared to controls (RCH and PCV). **e** GO terms enriched from a comparison among the libraries of VSB-30 flight-exposed tissues



these sequences were cross-referenced against the *Z. mays* database, another monocot plant. The identified pathway matches were as follows: (a) signaling pathway: inositol monophosphatase—*C5YT78\_SORBI* gene (94.6% identity to *Z. mays*—*B6T613\_MAIZE*), *C5YT79\_SORBI* gene (89.9% identity to *Z. mays*—*C0PES7\_MAIZE*), putative nucleoside phosphatase *C5WYL6\_SORBI* gene (90.9% sequence identical to *Z. mays*—*B4FWF1\_MAIZE*); (b) plant metabolism: pyruvate kinase *C5WRD4\_SORBI* (*SORBI\_3001G290600*), pyruvate kinase *C5WPQ9\_SORBI* (*SORBI\_3001G140700*), phosphoglycolate phosphatase 1a chloroplastic—*C5YBC8\_SORBI* gene (91.5% identical to *Z. mays*—*B4FPG9\_MAIZE*), 4-hydroxy-3-methyl but-2-enyl diphosphate reductase—*C5WLY2\_SORBI* gene (95.9% sequence identical to *Z. mays*—*C0PDR3\_MAIZE*), methylcrotonoyl-coa carboxylase beta chain mitochondrial—*C5YL06\_SORBI* gene (94.9% sequence identical to *B6SWZ4\_MAIZE*), glyco\_hydro 19—*C5WZU7\_SORBI*, glyco\_hydro 18—*C5XQ18\_SORBI* and *C5Y5V0\_SORBI*, aldedh domain-containing protein—*C5YLK6\_SORNI*, chlorophyll a-b binding protein—*C5WTC1\_SORBI*; (c) DNA/RNA/protein synthesis—translation initiation factor eif-2b alpha subunit—*A0A1Z5R6U1\_SORBI* gene (95.4% sequence identity to *B6TJL9\_MAIZE*), importin protein—*C5YWA7*, cp-type domain protein—*C5YSD9\_SORBI*, DNA helicase—*C5XMX5\_SORBI*, DNA repair rad51—*C5YNU8\_SORBI*; (d) associated to hormone: abscisic acid 8'-hydroxylase-3—*C5YMA6\_SORBI* gene (83.4% sequence identical to *K7UTR6\_MAIZE*), abscisic acid 8—*C5X2B0\_SORBI* gene (88.6% sequence identical to *Panicum miliaceum*—*A0A3L6T6J4\_PANMI*); and (e) associated to stress—inhibitor of striate1—*C5Z498\_SORBI* gene (92.0% identical to *A0A1D6JD24\_MAIZE*), methionine

gamma-lyase—*C5WVD4\_SORBI* gene (89.3% sequence identical to *A0A1D6GMP0\_MAIZE*) (Table 3).

Considering this information, we constructed a schematic representation of these genes and their associated pathways to provide a concise summary of the findings and to enhance our understanding of how sugarcane plants might respond to the VSB-30 flight (Fig. 7).

## Discussion

As a relatively nascent field of research, space agriculture raises numerous inquiries regarding plant perception, response, plant development, and yield, particularly in the context of altered gravitational conditions (Paul et al. 2012; Hoson 2014; Zheng et al. 2015; Zhu 2016; Beisel et al. 2019; Kruse et al. 2020; Sathasivam et al. 2021; Baba et al. 2022). Nevertheless, the primary plant models employed in these investigations have been *Arabidopsis* seedlings or callus, rice, or maize roots (Zhang et al. 2015; Sathasivam et al. 2021). To broaden our understanding of plant response in such conditions, we examined 10-day-old sugarcane plants—a monocot with C4 metabolism, accompanied by available transcriptome and partial genome data (Vettore et al. 2001; de Setta et al. 2014). We subjected these plants to abrupt shifts in gravitational forces using the VSB-30 sounding rocket.

The duration of altered gravity exposure significantly triggered transformative changes in sugarcane tissue organization, as indicated by our histological findings. These results demonstrated the disruption of xylem and phloem arrangement in leaf tissues of vertically and horizontally positioned plants. Analogous morphological alterations were observed

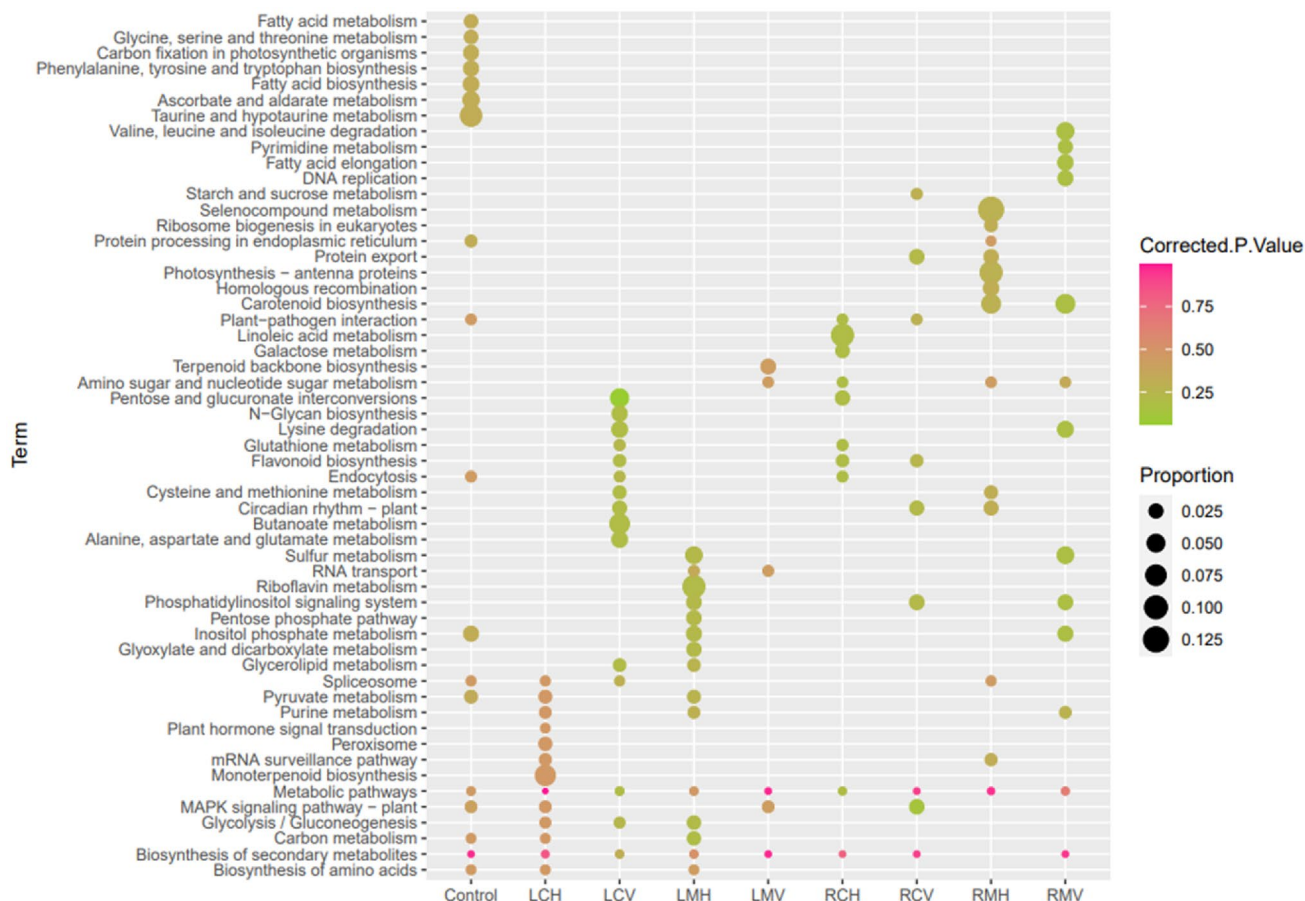


**Fig. 6** Enriched metabolic pathways. The chart illustrates the distribution of genes linked to enriched metabolic pathways across the PCV (Control), LCH, LCV, LMH, LMV, RCH, RCV, RMH, and RMV libraries. Dot sizes correspond to the ratio of genes within the enriched metabolic pathway to the total genes within that pathway. The color gradient indicates significance levels (corrected *p*-values): Pink (0.75) signifies higher significance, while green (0.25) indicates lower significance. *LCH* Leaves control in horizontal position, *LCV*

Leaves control in vertical position, *RCH* Roots control in horizontal position, *RCV* Roots control in vertical position, *PCV* Plantlets submitted to control shaker, *LMH* Leaves VSB-30 flight-submitted in horizontal position, *LMV* Leaves VSB-30 flight-submitted in vertical position, *RMH* Roots VSB-30 flight-submitted in horizontal position, *RMV* Roots VSB-30 flight-submitted in vertical position (Color figure online)

by Hoson (2014) in rice, where modifications in coleoptile growth and expansion pattern were documented. Soga et al. (2018) also proposed that changes in tissue organization might serve as a mechanism by which plants counteract shifts in gravitational forces.

Another noteworthy alteration identified through histological analysis of sugarcane was the accumulation of lignin within the epidermal and Kranz regions of leaves. The lignin accumulation coincided with heightened levels of  $H_2O_2$  and could be attributed to the elevated activities of POX and SOD observed in leaves. The conversion of  $H_2O_2$  to  $H_2O$  by plant POXs and SODs entails an electron transfer to monolignol, which subsequently contributes to lignin formation (Tsukagoshi 2016). The biochemical data presented here indicated elevated SOD and POX activity in leaves, thereby reinforcing the observed lignin accumulation in histological

analysis. Similar alterations in cell wall structure were also observed in *Arabidopsis* callus cultures (Fengler et al. 2015, 2016) and *Arabidopsis petioles* (Johnson et al. 2015) when exposed to gravitational changes. This modification appears to be a recurrent response to plant abiotic stress (Paul et al. 2012; Hoson and Wakabayashi 2015; Baba et al. 2022). Furthermore, upon restoring normal growth conditions to 1 g aM plants, histological analysis revealed a reorganization of vascular bundles in leaf tissues, although the lignin accumulation persisted. According to Sharma et al. (2022), plants might develop a stress memory that alters their physiological, metabolic, and epigenetic responses to tolerate such fluctuations. With regard to microgravity, this area still requires further elucidation.

The transcriptome analysis revealed significant changes in enriched pathways in both roots and leaves. Based on

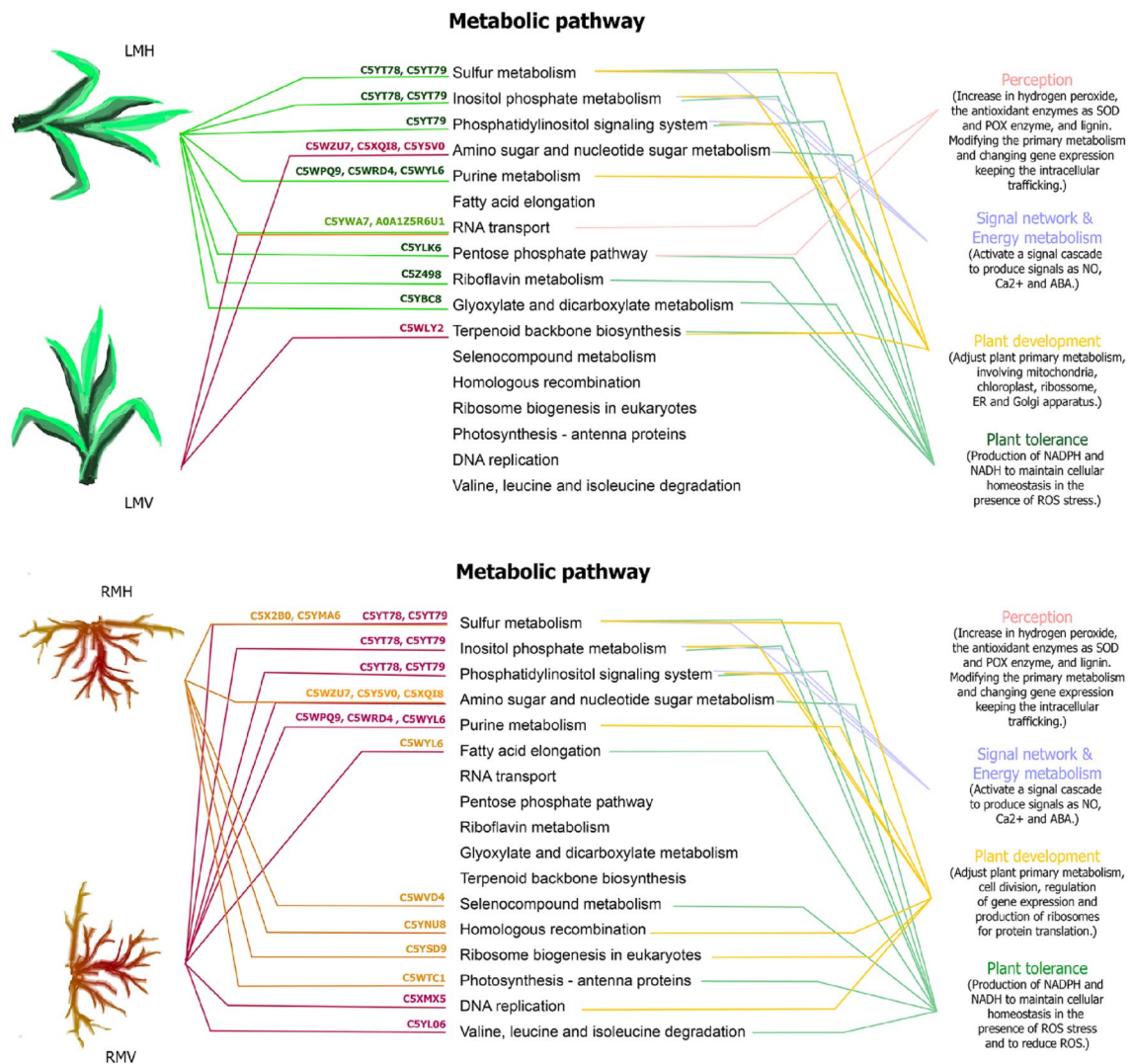
**Table 3** Genes identified within distinct or overlapping pathways in sugarcane RNA-seq libraries

Entry	Sequence homology	Sequence code	Protein name	Arabidopsis database (TAIR)	Pathways (libraries identified)
<i>C5YT78_SORBI</i>	Uncharacterized protein	<i>B6T613_MAIZE</i> (94.6%)	Inositol monophosphatase family protein	<i>AT5G63980</i>	Sulfur metabolism (LMH/RMV) Phosphatidylinositol signaling system (LMH/RMV) Inositol phosphate metabolism (LMH/RMV)
<i>C5YT79_SORBI</i>	Uncharacterized protein	<i>C0PES7_MAIZE</i> (89.9%)	Diphosphonucleotide phosphatase1	<i>AT5G63980</i>	Sulfur metabolism (LMH/RMV) Phosphatidylinositol signaling system (LMH/RMV) Inositol phosphate metabolism (LMH/RMV)
<i>C5WZU7_SORBI</i>	Glyco_hydro_19_cat domain-containing protein			<i>AT1G02360</i>	Amino sugar and nucleotide sugar metabolism (LMV/RMH/RMV)
<i>C5XQI8_SORBI</i>	Glyco_hydro_18 domain-containing protein			<i>AT5G24090</i>	Amino sugar and nucleotide sugar metabolism (LMV/RMH/RMV)
<i>C5Y5V0_SORBI</i>	Glyco_hydro_18 domain-containing protein				Amino sugar and nucleotide sugar metabolism (LMV/RMH/RMV)
<i>C5WYL6_SORBI</i>	Uncharacterized protein)	<i>B4FWF1_MAIZE</i> (90.9%)	Putative nucleoside phosphatase gda1/cd39 family protein	<i>AT1G14250</i>	Purine metabolism (RMV/LMH) Fatty acid elongation (RMV)
<i>C5WRD4_SORBI</i>	Pyruvate kinase (ec 2.7.1.40)			<i>AT1G32440</i>	Purine metabolism (RMV/LCH/LMH)
<i>C5WPQ9_SORBI</i>	Pyruvate kinase (ec 2.7.1.40)			<i>AT3G22960</i>	Purine metabolism (RMV/LMH)
<i>A0A1Z5R6U1_SORBI</i>	Uncharacterized protein	<i>B6TJL9_MAIZE</i> (95.4%)	Translation initiation factor eif-2b alpha subunit	<i>AT1G72340</i>	RNA transport (LMH/LMV)
<i>C5YWA7_SORBI</i>	Importin n-terminal domain-containing protein			<i>AT3G08947</i>	RNA transport (LMH/LMV)
<i>C5YMA6_SORBI</i>	Uncharacterized protein	<i>K7UTR6_MAIZE</i> (83.4%)	Abscisic acid 8'-hydroxylase-3	<i>AT3G19270</i>	Sulfur metabolism (RMH/RMV)
<i>C5X2B0_SORBI</i>	Uncharacterized protein	<i>A0A3L6T6J4_PANMI</i> (88.6%)	Abscisic acid 8	<i>AT3G19270</i>	Sulfur metabolism (RMH/RMV)
<i>C5YLK6_SORBI</i>	Aldedh domain-containing protein			<i>AT2G24270</i>	Pentose phosphate pathway (LMH)
<i>C5Z498_SORBI</i>	Uncharacterized protein	<i>A0A1D6JD24_MAIZE</i> (92.0%)	Inhibitor of striate1	<i>AT4G11570</i>	Riboflavin metabolism (LMH)
<i>C5YBC8_SORBI</i>	Uncharacterized protein	<i>B4FPG9_MAIZE</i> (91.5%)	Phosphoglycolate phosphatase 1a chloroplastic	<i>AT5G47760</i>	Glyoxylate and dicarboxylate metabolism (LMH)
<i>C5WLY2_SORBI</i>	Uncharacterized protein	<i>C0PDR3_MAIZE</i> (95.9%)	4-hydroxy-3-methylbut-2-enyl diphosphate reductase	<i>AT4G34350</i>	Terpenoid backbone biosynthesis (LMV)
<i>C5WVD4_SORBI</i>	Uncharacterized protein	<i>A0A1D6GMP0_MAIZE</i> (89.3%)	Methionine gamma-lyase	<i>AT1G64660</i>	Seleno-compound metabolism (RMH)



**Table 3** (continued)

Entry	Sequence homology	Sequence code	Protein name	Arabidopsis database (TAIR)	Pathways (libraries identified)
<i>C5YNU8_SORBI</i>	DNA repair protein rad51 homolog			<i>AT5G20850</i>	Homologous recombination (RMH)
<i>C5YSD9_SORBI</i>	cp-type g domain-containing protein			<i>AT1G08410</i>	Ribosome biogenesis in eukaryotes (RMH)
<i>C5WTC1_SORBI</i>	Chlorophyll a-b binding protein, chloroplastic			<i>AT2G05100</i>	Photosynthesis—antenna proteins (RMH)
<i>C5XMX5_SORBI</i>	DNA helicase			<i>AT2G16440</i>	DNA replication (RMV)
<i>C5YL06_SORBI</i>	Uncharacterized protein	<i>B6SWZ4_MAIZE</i> (94.9%)	Methylcrotonoyl-coa carboxylase beta chain mitochondrial	<i>AT4G34030</i>	Valine, leucine, and isoleucine degradation (RMV)

**Fig. 7** Summary of the functional profile derived from the transcripts linked to enriched metabolic pathways in VSB-30 flight-exposed libraries

this data, it can be proposed that sugarcane plants detected alterations in gravitational force and subsequently translated perception into changes in the expression of the Phosphatidylinositol and Inositol pyrophosphate pathways. These pathways are recognized as a family of signaling molecules involved in various cellular processes associated with signal network and energy metabolism. Kriegs et al. (2006), Martzivanou et al. (2006) and Salinas-Mondragon et al. (2010) have suggested that these two pathways might be responsible for perceiving changes in gravitational forces. Moreover, the Phosphatidylinositol and Inositol pyrophosphate pathways may be directly or indirectly linked to the cellular redox response, potentially inducing the Sulphur metabolism pathway. This could lead to alterations in the expression of various proteins such as kinases, phosphatases, and peroxidases, all contributing to the maintenance of cellular redox homeostasis (Martzivanou et al. 2006; Barjaktarović et al. 2007; Fengler et al. 2015; Zhang et al. 2015; Fengler et al. 2016; Baba et al. 2022).

Other pathways shared between roots and leaves, such as purine metabolism, play a crucial role in fine-tuning plant primary metabolism. These pathways involve critical cellular components including mitochondria, chloroplast, ribosome, endoplasmic reticulum (ER), and Golgi apparatus. They collectively contribute to sustaining plant development within these novel conditions (Zhang et al. 2015; Kruse et al. 2020; Sathasivam et al. 2021).

Additionally, our findings also underscored pathways specific to leaves and roots. In leaves, the observed alterations in metabolic pathways are linked to the pentose phosphate pathway, which serves as source of reduced NADPH to maintain cytosolic reduced glutathione levels, particularly crucial under heightened ROS scenarios his pathway plays a role in connecting chloroplast, mitochondria, and cytosol (Hou and Bartels 2015; Sharkey 2021). Notably, similar differential gene and protein expression associated with primary metabolism and photosynthesis has been observed in *Arabidopsis* cell cultures or plants exposed to simulated or actual microgravity (Barjaktarović et al. 2007; Martzivanou et al. 2006; Zhang et al. 2015; Salinas-Mondragon et al. 2010; Fengler et al. 2015, 2016; Baba et al. 2022). In the sugarcane leaf tissue libraries, transcripts related to riboflavin metabolism and terpenoid pathways were identified. Deng et al. (2014) proposed that riboflavin might play a pivotal and ambivalent role in abiotic stress, inducing tolerance low levels while potentially affecting plant tolerance at high levels. The reactions in the riboflavin pathway interconnect to fatty acid oxidation, FMN, FAD production, as well as ROS-related reactions. On the other hand, terpenoid pathways are integral to secondary plant metabolism, contributing to plant defense, development, and stress responses (Tholl 2015; Fengler et al. 2015, 2016; Zhang

et al. 2015; Zheng et al. 2015; Mao et al. 2019; Kruse et al. 2020; Sathasivam et al. 2021).

A pathway exclusive to the root libraries was the Seleno-compound metabolism. Selenium, an essential micronutrient, not only exhibits antioxidant activity but also enhances plant resilience to abiotic conditions by influencing chromatin remodeling and gene expression regulation (Dou et al. 2021). Moreover, transcripts from pathways linked to valine–leucine and isoleucine degradation were detected in the root libraries. These pathways are integral to amino acid degradation metabolism, maintaining cellular energy and amino acid pool homeostasis. Certain amino acids or their derivatives, such as proline, glycine, and glycine-betaine, also serve as osmoprotectants and antioxidants (Sánchez-Bermúdez et al. 2022), with amino acid pathways often interconnected. Consequently, heightened flux or gene expression associated with these pathways is a common response to various abiotic stressors (Gipson et al. 2017; Huang and Jander 2017). This dataset raises a hypothesis regarding how sugarcane roots may perceive and respond to gravitational force changes. This modification could potentially trigger the Seleno-compound pathway, while valine–leucine and isoleucine degradation might provide root cells with molecules having antioxidant properties, thereby maintaining redox homeostasis and promoting stress tolerance. Achieving this could entail specific gene expression regulation, ribosome biogenesis, and the preservation of DNA metabolism through DNA replication and repair. These processes are pivotal for cell division preparation, a vital aspect of plant growth (Barjaktarović et al. 2007; Jeon et al. 2015; Zhao et al. 2015; Roy and Das 2017; Sathasivam et al. 2021). Zhang et al. (2015) observed robust microgravity cultivation, characterized by subtle yet continuous cell division. Similarly, Fengler et al. (2015) noted comparable results in callus tissues maintained during a spaceflight for 5 days. These findings are in alignment with our hypothesis, suggesting that sugarcane roots may indeed be priming themselves for cell division.

Surprisingly, transcripts linked to photosynthesis and antenna proteins were found in the root tissue libraries. These sequences could indicate a response to whole-tissue reprogramming prompted by the absence of light during the VSB-30 flight and until payload recovery. Alternatively, they might be associated with the synthesis of electron donor/acceptor molecules necessary for adapting to altered redox homeostasis. Some of these molecules could potentially activate chromatin-remodeling factors, enabling the expression of genes aimed at managing excess ROS (Damkjær et al. 2009; Pietrzykowska et al. 2014; Sharma et al. 2022).

It's important to emphasize that a portion of the transcriptional response is only partially linked to changes in gravitational force (hypergravity and microgravity). The experiment introduced other stress-inducing conditions to the sugarcane

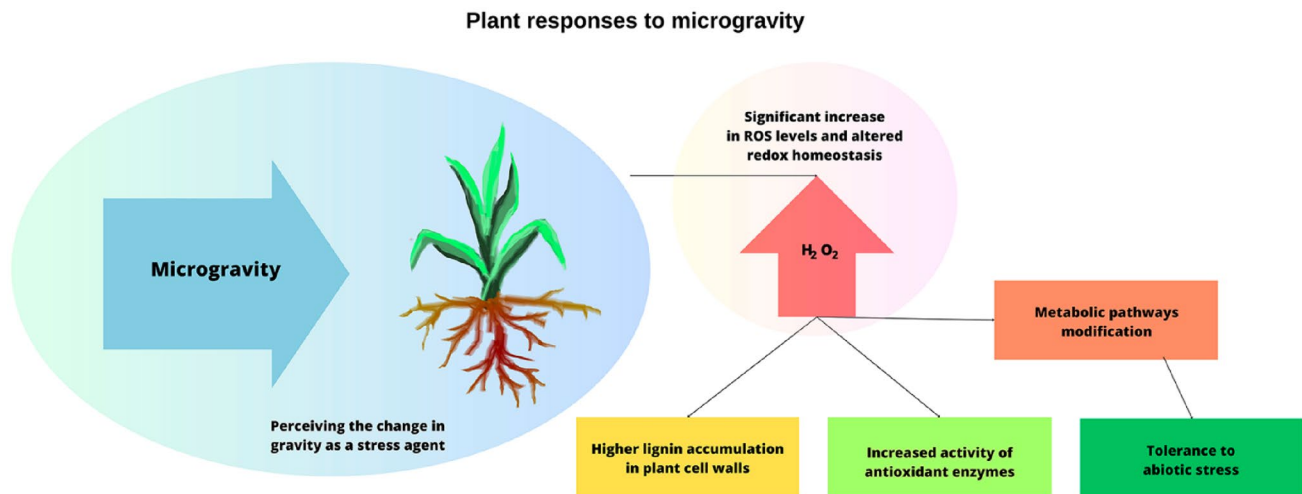


**Fig. 8** Modeling how sugarcane responds to changes in gravitational force

plants, including vibration, rotation, sound, darkness, short-term hypoxia, and substrate changes. Similarly, both field conditions and controlled experimental settings often subject plants to various combined stress scenarios (Mittler 2006; Sánchez-Bermúdez et al. 2022).

The available proteomic, microarray, and transcriptome data for *Arabidopsis* models (petioles, plants, cells, or callus), combined with the findings presented here for sugarcane, suggest that the Phosphatidylinositol and Inositol pyrophosphate pathways could serve as a pivotal route in perceiving gravitational force changes. Additionally, the cascade effect of the pathways could trigger or suppress other pathways, such as the sulfur metabolism pathway, peroxidase enzymes, kinases and phosphatase enzymes, pentose phosphate pathway, ribosomal proteins biosynthesis,  $Ca^{2+}$ , auxin transport, carbohydrate metabolism, lipid metabolism, photosynthesis, respiratory electron transport proteins, DNA repair, DNA replication, and cell division, among others. These modifications contribute to plant tolerance, helping to adjust cellular homeostasis to new condition and facilitating development even under adverse circumstances (Martizanou et al. 2006; Barjaktarović et al. 2007; Salinas-Mondragon et al. 2010; Paul et al. 2012; Fengler et al. 2015; Zhang et al. 2015; Fengler et al. 2016; Zheng et al. 2015; Zhu 2016; Chen and Heidari 2020; Baba et al. 2022; Narayan et al. 2022).

Furthermore, these results align with physiological and biochemical analyses, where the identified genes can be associated with metabolic pathways, enabling the understanding of how changes in gravitational force impact redox homeostasis in sugarcane plants, directly influencing their development. In conclusion, this study serves as a foundational platform for comprehending how sugarcane responds to such stress conditions. It can guide future research for

developing plant varieties resistant to adverse circumstances, expanding knowledge of plant responses to abrupt and combined environmental changes, optimizing agricultural productivity, and enhancing techniques for cultivating plants in space (Fengler et al. 2015; Johnson et al. 2015; Zheng et al. 2015; Faraoni et al. 2019; Sathasivam et al. 2021; Baba et al. 2022).

## Conclusions

In summary, our study enhances our understanding of how plants respond to alterations in gravitational forces using a C4 monocot plant. We observed changes in redox homeostasis across both root and leaf tissues, evident histological levels (tissue organization and lignin accumulation), biochemical levels (SOD and POX activity), and transcriptional levels through the identification of various pathways. Key insights garnered from this research emphasize the significance of the phosphatidylinositol and inositol pyrophosphate pathways as crucial signaling routes for perception, translating into diverse cascades that impact tissue organization, redox homeostasis, and alterations in plant metabolism (Fig. 8). These changes involve modifications in photosynthesis, pentose metabolism, amino acid pathways, DNA replication, DNA repair, and other genes/protein, collectively contributing to the plant's ability to mitigate the effect of such changes, tolerate adverse conditions, and maintain the developmental processes. The implications of these findings expand the scope of knowledge within this research domain. This newfound understanding holds relevance for advancing crop development and improving yields both in space and under diverse abiotic conditions here on Earth.



**Supplementary Information** The online version contains supplementary material available at <https://doi.org/10.1007/s00344-023-11149-y>.

**Acknowledgements** We wish to express our gratitude to USINA ESTIVAS—BIOSEV for providing the sugarcane plants and to the teams from CLBI, CLA, and AEB for their invaluable support during the Maracati II mission. Additionally, we extend our thanks to Flávio Correia-Junior F. and Gualberto-Junior J., for the helpful suggestions and assistance in the development of the boxes utilized in the Maracati II mission. The authors would also like to acknowledge the technical support provided by the High-Performance Computing Center at UFRN (NPAD/UFRN).

**Author Contributions** HCS and KCS participated in the Maracati II mission, HCS and KFMB made the biochemical and histological assays; LFS, VVN, and DGT worked with RNA-seq data. KCS contributed to conceptualization and design of the work; KCS and JPMSS wrote a first draft of the manuscript; and all authors contributed to and agreed upon the final version.

**Funding** “This research was funded by Agência Espacial Brasileira (AEB), FINEP, CAPES, Financial code 01; INCT- CNPQ/INESPAÇO. Helaine Cristiane Silva, Diego Gomes Teixeira, Vladimir Vieira do Nascimento; Kellya Francisca Mendonça Barreto were recipients of scholarship from CAPES; Katia C. Scortecci has a CNPq fellowship.”

**Data Availability** “Upon request,” RNA-seq data are available at BioProject ID PRJNA917241 (NCBI).

## Declarations

**Conflict of Interest** On behalf of all authors, the corresponding author affirms that there is no conflict of interest.

**Institutional Review Board Statement** “Not applicable.”

## References

- Baba AI, Mir MY, Riyazuddin R, Cséplő Á, Rigó G, Fehér A (2022) Plants in microgravity: molecular and technological perspectives. *Int J Mol Sci* 23:10548. <https://doi.org/10.3390/ijms231810548>
- Barjaktarović Ž, Nordheim A, Lamkemeyer T, Fladerer C, Madlung J, Hampp R (2007) Time-course of changes in amounts of specific proteins upon exposure to hyper-g, 2-D clinorotation, and 3-D random positioning of *Arabidopsis* cell cultures. *J Exp Bot* 58:4357–4363. <https://doi.org/10.1093/jxb/erm302>
- Barjaktarović Ž, Schütz W, Madlung J, Fladerer C, Nordheim A, Hampp R (2009) Changes in the effective gravitational field strength affect the state of phosphorylation of stress-related proteins in callus cultures of *Arabidopsis thaliana*. *J Exp Bot* 60:779–789. <https://doi.org/10.1093/jxb/ern324>
- Beisel NS, Noble J, Barbazuk WB, Paul A-L, Ferl RJ (2019) Spaceflight-induced alternative splicing during seedling development in *Arabidopsis thaliana*. *npj Microgravity* 5:1–5. <https://doi.org/10.1038/s41526-019-0070-7>
- Bradford MM (1976) A rapid and sensitive method for the quantitation of microgram quantities of protein utilizing the principle of protein-dye binding. *Anal Biochem* 72:248–254. <https://doi.org/10.1006/abio.1976.9999>
- Buchfink B, Xie C, Huson DH (2015) Fast and sensitive protein alignment using DIAMOND. *Nat Methods* 12:59–60. <https://doi.org/10.1038/nmeth.3176>
- Cavalcanti FR, Santos Lima JPM, Ferreira-Silva SL, Viégas RA, Silveira JAG (2007) Roots and leaves display contrasting oxidative response during salt stress and recovery in cowpea. *J Plant Physiol* 164:591–600. <https://doi.org/10.1016/j.jplph.2006.03.004>
- Chen J-T, Heidari P (2020) Cell signaling in model plants. *Int J Mol Sci* 21:6062. <https://doi.org/10.3390/ijms21176062>
- Damkjær JT, Kereiche S, Johnson MP, Kovacs L, Kiss AZ, Boekema EJ, Ruban AV, Horton P, Jansson S (2009) The photosystem II light-harvesting protein Lhcb3 affects the macrostructure of photosystem ii and the rate of state transitions in *Arabidopsis*. *Plant Cell* 21:3245–3256. <https://doi.org/10.1105/tpc.108.064006>
- de Setta N, Monteiro-Vitorello CB, Metcalfe CJ, Cruz GMQ, Del Bem LE, Vicentini R, Nogueira FTS, Campos RA, Nunes SL, Turcini PCG, Vieira AP, Ochoa Cruz EA, Corrêa TCS, Hotta CT, de Mello Varani A, Vautrin S, da Trindade AS, de Mendonça Vilela M, Lembke CG, Sato PM, de Andrade RF, Nishiyama MY, Cardoso-Silva CB, Scortecci KC, Garcia AAF, Carneiro MS, Kim C, Paterson AH, Bergès H, D’Hont A, de Souza AP, Souza GM, Vincentz M, Kitajima JP, Van Sluys M-A (2014) Building the sugarcane genome for biotechnology and identifying evolutionary trends. *BMC Genomics* 15:540. <https://doi.org/10.1186/1471-2164-15-540>
- Deng B, Jin X, Yang Y, Lin Z, Zhang Y (2014) The regulatory role of riboflavin in the drought tolerance of tobacco plants depends on ROS production. *Plant Growth Regul* 72:269–277. <https://doi.org/10.1007/s10725-013-9858-8>
- Dou L, Tian Z, Zhao Q, Xu M, Zhu Y, Luo X, Qiao X, Ren R, Zhang X, Li H (2021) Transcriptomic characterization of the effects of selenium on maize seedling growth. *Front Plant Sci* 12:737029. <https://doi.org/10.3389/fpls.2021.737029>
- Faraoni P, Sereni E, Gnerucci A, Cialdai F, Monici M, Ranaldi F (2019) Glyoxylate cycle activity in *Pinus pinea* seeds during germination in altered gravity conditions. *Plant Physiol Biochem* 139:389–394. <https://doi.org/10.1016/j.plaphy.2019.03.042>
- Fengler S, Spierer I, Neef M, Ecke M, Nieselt K, Hampp R (2015) A whole-genome microarray study of *Arabidopsis thaliana* semi-solid callus cultures exposed to microgravity and nonmicrogravity related spaceflight conditions for 5 days on board of Shenzhou 8. *Biomed Res Int* 2015:e547495. <https://doi.org/10.1155/2015/547495>
- Fengler S, Spierer I, Neef M, Ecke M, Hauslage J, Hampp R (2016) Changes in gene expression of *Arabidopsis thaliana* cell cultures upon exposure to real and simulated partial-g forces. *Microgravity Sci Technol* 28:319–329. <https://doi.org/10.1007/s12217-015-9452-y>
- Gipson AB, Morton KJ, Rhee RJ, Simo S, Clayton JA, Perrett ME, Binkley CG, Jensen EL, Oakes DL, Rouhier MF, Rouhier KA (2017) Disruptions in valine degradation affect seed development and germination in *Arabidopsis*. *Plant J* 90:1029–1039. <https://doi.org/10.1111/tpj.13538>
- Grabherr MG, Haas BJ, Yassour M, Levin JZ, Thompson DA, Amit I, Adiconis X, Fan L, Raychowdhury R, Zeng Q, Chen Z, Mauceli E, Hacohen N, Gnirke A, Rhind N, di Palma F, Birren BW, Nusbaum C, Lindblad-Toh K, Friedman N, Regev A (2011) Trinity: reconstructing a full-length transcriptome without a genome from RNA-Seq data. *Nat Biotechnol* 29:644. <https://doi.org/10.1038/nbt.1883>
- Hashiguchi Y, Tasaka M, Morita MT (2013) Mechanism of higher plant gravity sensing. *Am J Bot* 100:91–100. <https://doi.org/10.3732/ajb.1200315>
- Havir EA, McHale NA (1987) Biochemical and developmental characterization of multiple forms of catalase in tobacco leaves. *Plant Physiol* 84:450–455. <https://doi.org/10.1104/pp.84.2.450>
- Herranz R, Medina FJ (2014) Cell proliferation and plant development under novel altered gravity environments. *Plant Biol* 16:23–30. <https://doi.org/10.1111/plb.12103>

- Hoson T (2014) Plant growth and morphogenesis under different gravity conditions: relevance to plant life in space. *Life* 4:205–216. <https://doi.org/10.3390/life4020205>
- Hoson T, Wakabayashi K (2015) Role of the plant cell wall in gravity resistance. *Phytochemistry* 112:84–90. <https://doi.org/10.1016/j.phytochem.2014.08.022>
- Hou Q, Bartels D (2015) Comparative study of the aldehyde dehydrogenase (ALDH) gene superfamily in the glycophyte *Arabidopsis thaliana* and *Eutrema halophytes*. *Ann Bot* 115:465–479. <https://doi.org/10.1093/aob/mcu152>
- Huang T, Jander G (2017) Abscisic acid-regulated protein degradation causes osmotic stress-induced accumulation of branched-chain amino acids in *Arabidopsis thaliana*. *Planta* 246:737–747. <https://doi.org/10.1007/s00425-017-2727-3>
- Jeon Y, Park Y-J, Cho HK, Jung HJ, Ahn T-K, Kang H, Pai H-S (2015) The nucleolar GTPase nucleostemin-like 1 plays a role in plant growth and senescence by modulating ribosome biogenesis. *J Exp Bot* 66:6297–6310. <https://doi.org/10.1093/jxb/erv337>
- Johnson CM, Subramanian A, Edelmann RE, Kiss JZ (2015) Morphometric analyses of petioles of seedlings grown in a spaceflight experiment. *J Plant Res* 128:1007–1016. <https://doi.org/10.1007/s10265-015-0749-0>
- Kanehisa M, Goto S (2000) KEGG: Kyoto Encyclopedia of Genes and Genomes. *Nucleic Acids Res* 28:27–30. <https://doi.org/10.1093/nar/28.1.27>
- Kim D, Langmead B, Salzberg SL (2015) HISAT: a fast spliced aligner with low memory requirements. *Nat Methods* 12:357–360. <https://doi.org/10.1038/nmeth.3317>
- Kordyum EL (2014) Plant cell gravisensitivity and adaptation to microgravity. *Plant Biol* 16:79–90. <https://doi.org/10.1111/plb.12047>
- Kriegs B, Theisen R, Schnabl H (2006) Inositol 1, 4, 5-trisphosphate and Ran expression during simulated and real microgravity. *Protoplasma* 229:163–174. <https://doi.org/10.1007/s00709-006-0214-y>
- Kruse CPS, Meyers AD, Basu P, Hutchinson S, Luesse DR, Wyatt SE (2020) Spaceflight induces novel regulatory responses in *Arabidopsis* seedling as revealed by combined proteomic and transcriptomic analyses. *BMC Plant Biol* 20:1–16. <https://doi.org/10.1186/s12870-020-02392-6>
- Langdale JA (1994) In situ hybridization. In: Freeling M, Walbot V (eds) *The maize handbook*, Springer lab manuals. Springer, Berlin, pp 165–180. [https://doi.org/10.1007/978-1-4612-2694-9\\_18](https://doi.org/10.1007/978-1-4612-2694-9_18)
- Li H, Handsaker B, Wysoker A, Fennell T, Ruan J, Homer N, Marth G, Abecasis G, Durbin R, 1000 Genome Project Data Processing Subgroup (2009) The Sequence Alignment/Map format and SAMtools. *Bioinformatics* 25:2078–2079. <https://doi.org/10.1093/bioinformatics/btp352>
- Mao J, He Z, Hao J, Liu T, Chen J, Huang S (2019) Identification, expression, and phylogenetic analyses of terpenoid biosynthesis-related genes in secondary xylem of loblolly pine (*Pinus taeda* L.) based on transcriptome analyses. *PeerJ* 7:e6124. <https://doi.org/10.7717/peerj.6124>
- Martin M (2011) Cutadapt removes adapter sequences from high-throughput sequencing reads. *EMBnet journal* 17:10–12. <https://doi.org/10.14806/ej.17.1.200>
- Martzivanou M, Babbick M, Cogoli-Greuter M, Hampp R (2006) Microgravity-related changes in gene expression after short-term exposure of *Arabidopsis thaliana* cell cultures. *Protoplasma* 229:155–162. <https://doi.org/10.1007/s00709-006-0203-1>
- Medeiros NMC, Córdoba-Cañero D, García-Gil CB, Ariza RR, Roldán-Arjona T, Scortecci KC (2019) Characterization of an AP endonuclease from sugarcane—ScARP1. *Biochem Biophys Res Commun* 514:926–932. <https://doi.org/10.1016/j.bbrc.2019.04.156>
- Mittler R (2006) Abiotic stress, the field environment and stress combination. *Trends Plant Sci* 11:15–19. <https://doi.org/10.1016/j.tplants.2005.11.002>
- Morais ERDC, de Medeiros NMC, da Silva FL, de Sousa IAL, de Oliveira IGB, Meneses CHSG, Scortecci KC (2023) Redox homeostasis at SAM: a new role of HINT protein. *Planta* 257:12. <https://doi.org/10.1007/s00425-022-04044-5>
- Narayan OP, Kumar P, Yadav B, Dua M, Johri AK (2022) Sulfur nutrition and its role in plant growth and development. *Plant Signal Behav*. <https://doi.org/10.1080/15592324.2022.2030082>
- Patel RK, Jain M (2012) NGS QC toolkit: a toolkit for quality control of next generation sequencing data. *PLoS ONE* 7:e30619. <https://doi.org/10.1371/journal.pone.0030619>
- Paul A-L, Amalfitano CE, Ferl RJ (2012) Plant growth strategies are remodeled by spaceflight. *BMC Plant Biol* 12:232. <https://doi.org/10.1186/1471-2229-12-232>
- Pietrzykowska M, Suorsa M, Semchonok DA, Tikkanen M, Boekema EJ, Aro E-M, Jansson S (2014) The light-harvesting chlorophyll a/b binding proteins Lhcb1 and Lhcb2 play complementary roles during state transitions in *Arabidopsis*. *Plant Cell* 26:3646–3660. <https://doi.org/10.1105/tpc.114.127373>
- Roy S, Das KP (2017) Homologous recombination defective *Arabidopsis* mutants exhibit enhanced sensitivity to abscisic acid. *PLoS ONE* 12:e0169294. <https://doi.org/10.1371/journal.pone.0169294>
- Salinas-Mondragon RE, Kajla JD, Perera IY, Brown CS, Sederoff HW (2010) Role of inositol 1,4,5-triphosphate signalling in gravitropic and phototropic gene expression. *Plant Cell Environ* 33:2041–2055. <https://doi.org/10.1111/j.1365-3040.2010.02204.x>
- Sánchez-Bermúdez M, del Pozo JC, Pernas M (2022) Effects of combined abiotic stresses related to climate change on root growth in crops. *Front Plant Sci* 13:918537. <https://doi.org/10.3389/fpls.2022.918537>
- Sathasivam M, Hosamani R, Swamy BK, Kumaran GS (2021) Plant responses to real and simulated microgravity. *Life Sci Space Res* 28:74–86. <https://doi.org/10.1016/j.lssr.2020.10.001>
- Sayers EW, Bolton EE, Brister JR, Canese K, Chan J, Comeau DC, Connor R, Funk K, Kelly C, Kim S, Madej T, Marchler-Bauer A, Lanczycki C, Lathrop S, Lu Z, Thibaud-Nissen F, Murphy T, Phan L, Skripchenko Y, Tse T, Wang J, Williams R, Trzaskos BW, Pruitt KD, Sherry ST (2022) Database resources of the national center for biotechnology information. *Nucleic Acids Res* 50:D20–D26. <https://doi.org/10.1093/nar/gkab1112>
- Sharkey TD (2021) Pentose phosphate pathway reactions in photosynthesizing cells. *Cells* 10:1547. <https://doi.org/10.3390/cells10061547>
- Sharma M, Kumar P, Verma V, Sharma R, Bhargava B, Irfan M (2022) Understanding plant stress memory response for abiotic stress resilience: molecular insights and prospects. *Plant Physiol Biochem* 179:10–24. <https://doi.org/10.1016/j.plaphy.2022.03.004>
- Silva HC, Barreto K, Lima AK, Fonseca AC, Melo A, Gualberto-Junior J, Correa-Junior FA, Lemes G, Bastituzzo de Medeiros SR, Medeiros R, Scortecci KC (2011) Development of a system to submit sugarcane plants in real microgravity using the VSB30 sounding rocket. In: Ouwehand L (ed) *Proceedings of the 20th symposium on european rocket and balloon programmes and related research*, vol 700. ESA Communications, Noordwijk, pp 185–188
- Simão FA, Waterhouse RM, Ioannidis P, Kriventseva EV, Zdobnov EM (2015) BUSCO: assessing genome assembly and annotation completeness with single-copy orthologs. *Bioinformatics* 31:3210–3212. <https://doi.org/10.1093/bioinformatics/btv351>
- Soga K, Wakabayashi K, Hoson T (2018) Growth and cortical microtubule dynamics in shoot organs under microgravity and hypergravity conditions. *Plant Signal Behav* 13:e1422468. <https://doi.org/10.1080/15592324.2017.1422468>
- The UniProt Consortium (2022) UniProt: the universal protein knowledgebase in 2023. *Nucleic Acids Res* 51:D523–D531. <https://doi.org/10.1093/nar/gkac1052>

- Tholl D (2015) Biosynthesis and biological functions of terpenoids in plants. In: Schrader J, Bohlmann J (eds) *Biotechnology of isoprenoids, advances in biochemical engineering/biotechnology*. Springer International Publishing, Cham, pp 63–106. [https://doi.org/10.1007/10\\_2014\\_295](https://doi.org/10.1007/10_2014_295)
- Tian F, Yang D-C, Meng Y-Q, Jin J, Gao G (2020) PlantRegMap: charting functional regulatory maps in plants. *Nucleic Acids Res* 48:D1104–D1113. <https://doi.org/10.1093/nar/gkz1020>
- Torres TM, da Silva IB, de Castro ECP, dos Santos EA, da Cunha RMS, Lima JPMS (2014) Catalase inhibition affects glyoxylate cycle enzyme expression and cellular redox control during the functional transition of sunflower and safflower seedlings. *J Plant Growth Regul* 33:272–284. <https://doi.org/10.1007/s00344-013-9369-x>
- Tsukagoshi H (2016) Control of root growth and development by reactive oxygen species. *Curr Opin Plant Biol Growth Dev* 29:57–63. <https://doi.org/10.1016/j.pbi.2015.10.012>
- Ueda J, Miyamoto K, Uheda E, Oka M, Yano S, Higashibata A, Ishioka N (2014) Close relationships between polar auxin transport and graviresponse in plants. *Plant Biol* 16:43–49. <https://doi.org/10.1111/plb.12101>
- Urbanek H, Kuzniak-Gebarowska E, Herka K (1991) Elicitation of defence responses in bean leaves by *Botrytis cinerea* polygalacturonase. *Acta Physiol Plant* 13:43–50
- Vandenbrink JP, Kiss JZ, Herranz R, Medina FJ (2014) Light and gravity signals synergize in modulating plant development. *Front Plant Sci* 5:563. <https://doi.org/10.3389/fpls.2014.00563>
- Vettore AL, da Silva FR, Kemper EL, Arruda P (2001) The libraries that made SUCEST. *Genet Mol Biol* 24:1–7. <https://doi.org/10.1590/S1415-47572001000100002>
- Wickham H (2016) Data analysis. In: Wickham H (ed) *Ggplot2: elegant graphics for data analysis, use R!* Springer International Publishing, Cham, pp 189–201. [https://doi.org/10.1007/978-3-319-24277-4\\_9](https://doi.org/10.1007/978-3-319-24277-4_9)
- Wingett SW, Andrews S (2018) FastQ screen: a tool for multi-genome mapping and quality control. *F1000Res* 7:1338. <https://doi.org/10.12688/f1000research.15931.2>
- Xie C, Mao X, Huang J, Ding Y, Wu J, Dong S, Kong L, Gao G, Li C-Y, Wei L (2011) KOBAS 2.0: a web server for annotation and identification of enriched pathways and diseases. *Nucleic Acids Res* 39:W316–W322. <https://doi.org/10.1093/nar/gkr483>
- Zdobnov EM, Kuznetsov D, Tegenfeldt F, Manni M, Berkeley M, Kriventseva EV (2021) OrthoDB in 2020: evolutionary and functional annotations of orthologs. *Nucleic Acids Res* 49:D389–D393. <https://doi.org/10.1093/nar/gkaa1009>
- Zhang Y, Wang L, Xie J, Zheng H (2015) Differential protein expression profiling of *Arabidopsis thaliana* callus under microgravity on board the Chinese SZ-8 spacecraft. *Planta* 241:475–488. <https://doi.org/10.1007/s00425-014-2196-x>
- Zhao H, Lü S, Li R, Chen T, Zhang H, Cui P, Ding F, Liu P, Wang G, Xia Y, Running MP, Xiong L (2015) The *Arabidopsis* gene DIG6 encodes a large 60S subunit nuclear export GTPase 1 that is involved in ribosome biogenesis and affects multiple auxin-regulated development processes. *J Exp Bot* 66:6863–6875. <https://doi.org/10.1093/jxb/erv391>
- Zheng HQ, Han F, Le J (2015) Higher plants in space: microgravity perception, response, and adaptation. *Microgravity Sci Technol* 27:377–386. <https://doi.org/10.1007/s12217-015-9428-y>
- Zhu J-K (2016) Abiotic stress signaling and responses in plants. *Cell* 167:313–324. <https://doi.org/10.1016/j.cell.2016.08.029>

**Publisher's Note** Springer Nature remains neutral with regard to jurisdictional claims in published maps and institutional affiliations.

Springer Nature or its licensor (e.g. a society or other partner) holds exclusive rights to this article under a publishing agreement with the author(s) or other rightsholder(s); author self-archiving of the accepted manuscript version of this article is solely governed by the terms of such publishing agreement and applicable law.